Effect of nitric oxide on DNA repair dioxygenase – human AlkB homolog 2

BY

YULIYA MIKHED

B.Sc., National University “Lvivska Politechnika”, Ukraine, 2008

THESIS

Submitted as partial fulfillment of the requirements
for the degree of Master of Science in Medicinal Chemistry
in the Graduate College of the
University of Illinois at Chicago, 2012

Chicago, Illinois

Defense Committee:

Douglas D. Thomas, Chair and Advisor
Gregory R. Thatcher
Joanna E. Burdette

This thesis is dedicated to my mother, Svitlana Mikhed, without whom I would never be able to achieve what I have today.

ACKNOWLEDGMENTS

I will always feel a debt of gratitude for all people that have kindly provided me help during my graduate studies in the Department of Medicinal Chemistry and Pharmacognosy, College of Pharmacy, University of Illinois at Chicago. I couldn't have achieved my goals without them.

First of all, I would like to thank my advisor, Dr. Douglas D. Thomas for his guidance, support and encouragement during my study and research work. I feel enormously lucky to work with him during these three years. He was always there ready to help me out of any problem that occurred in my research work and encouraged me to overcome any challenge involved in my career. At the same time I always knew that I can seek an advice from him in my personal and professional growth.

I am very grateful to the members of my thesis defense committee – Dr. Gregory R. Thatcher and Dr. Joanna E. Burdette for their critical review of this thesis and continuous guidance throughout my studies.

I owe my deepest gratitude to Dr. Jason R. Hickok for his incredible help in all my research work in Dr. Thomas lab. Without his constant guidance in every research activity of mine I wouldn't be able to be where I am right now. I'm enormously thankful to Dr. Hickok for all the skills that he trained in me and for all the knowledge and experience that he shared.

I would like to extend my gratitude to Dr. Joanna E. Burdette for the opportunity to work in her lab during my rotation and for the extensive knowledge I was able to gain there, which I'm sure will be of great value in my future scientific career. I also would like to thank previous and

current members of her lab: Dr. Shelby M. King, Tyvette Hilliard, May Fern Toh, Suzanne Quartuccio, Amanda Muehlbauer, Roshan Ahmed, Dr. Kristine Ansenberger.

As well, I would like to thank Dr. Andrew Mesecar for giving me a chance to work in his lab for my rotation and obtain a practical experience in a big variety of research skills.

I am very thankful to Dr. Sumit Sahni for his help and advice during my work in Dr. Thomas lab. As well, I would like to thank all other lab members: Divya Vasudevan, Akanksha Arvind and Gaurang Bhide for their support and encouragement.

I'm thankful to the members of Dr. Petukhov group, especially to Hazem Abdelkarim for the tremendous impact he made in my life. I knew that I could always rely on him and without his help I would never be able to finish this thesis. As well, I would like to thank Emma L. Mendonca and Dr. Raghupati Neelarapu for all the help and advices that they supported me with during my research and studies.

As well, I would like to thank members of Dr. Bolton/Dr. Thatcher lab: Atieh Hajirahimkhan, Dr. Birgit M. Dietz, Madhubhani Hemachandra and others.

And last but not the least, I would like to say great thanks to my mother, Svitlana Mikhed, for constant motivation and encouragement to achieve everything that I have in life.

YM

TABLE OF CONTENTS

TABLE OF CONTENTS (continued)

LIST OF FIGURES

FIGURE PAGE

LIST OF ABBREVIATIONS

1-meA	1-methyl adenine
1-medAMP	1-methyldeoxyadenosine 5′-monophosphate
3-meA	3-methyl adenine
3-meC	3-methyl cytosine
5-meC	5-methyl cytosine
7-meG	7-methyl guanine
Akt	Protein kinase B
AlkB	Escherichia coli alkylation repair gene B
AP	Apurinic/apyrimidinic
Arg	Arginine amino acid
Asp	Aspartic acid
ATP	Adenosine-5'-triphosphate
BER	Base Excision Repair
cGMP	Cyclic guanosine monophosphate
CIP	Chelatable iron pool
DMEM	Dulbecco's Modified Eagle's cell culture medium

LIST OF ABBREVIATIONS (continued)

DNA	Deoxyribonucleic acid
DNIC	Dinitrosyl iron complexes
DNMT1	DNA Methyltransferase 1
DNMT3	DNA Methyltransferase 3
DNMT3A	DNA Methyltransferase 3 A
DNMT3B	DNA Methyltransferase 3 B
DNMT3L	DNA Methyltransferase 3 Like
dNTP	Deoxyribonucleotide triphosphate
DRR	Direct Reversal Pathway
dsDNA	Double stranded DNA
E.coli	Escherichia coli
EDTA	Ethylenediaminetetraacetic Acid
EPR	Electron paramagnetic resonance spectroscopy
ERK	Extracellular signal regulated kinase
FBS	Fetal bovine serum
GSH	Glutathione

LIST OF ABBREVIATIONS (continued)

hABH(1-8)	Human AlkB homologue 1-8
HeLa cells	Immortal cell line derived from cervical cancer cells
HIF-1α	Hypoxia inducible factor 1 α
His	Histidine amino acid
MBD4	Methyl-CpG binding protein 4
MGMT	O6-Methylguanine-DNA Methyltransferase
MMS	Methyl methanesulfonate
mRNA	Messenger RNA
NER	Nucleotide Excision Repair
NO·	Nitric oxide (free radical)
NONOate	Compound (R1R3N-(NO−)-N=O), where R1 and R2 are alkyl groups
O^{2-}	Superoxide
*O*4-meT	O4-methyl thymine
*O*6-meG	O6-methyl guanine
P (1-3)	Primers 1 - 3
P/S	Penicillin - Streptomycin

LIST OF ABBREVIATIONS (continued)

p53	Tumor protein 53
PARP	Poly ADP ribose polymerase
PBS	Phosphate buffered saline
PCHRV	Proline – Cysteine – Histidine – Arginine – Valine sequence of the amino acids
PCNA	Proliferating Cell Nuclear Antigen
PCR	Polymerase Chain Reaction
Phe	Phenylalanine amino acid
qRT-PCR	Quantitative Real Time Polymerase Chain Reaction
RKK	Arginine – Lysine – Lysine sequence of amino acids
RNA	Ribonucleic acid
RNOS	Reactive nitrogen oxide species
RPMI-1640	Roswell Park Memorial Institute cell culture medium
SDS	Sodium dodecyl sulfate
SEM	Standard Error of the Mean
S_N1	Nucleophilic substitution 1
S_N2	Nucleophilic substitution 2

LIST OF ABBREVIATIONS (continued)

Sper/NO	Spermine NONOate
ssDNA	Single stranded DNA
TAE	Tris Base, Glacial Acetic acid and EDTA buffer
TDG	Thymine glycosylase

SUMMARY

DNA methylation is a regulatory epigenetic process that is involved in gene silencing, genomic imprinting and X-chromosome inactivation. Aberrant states of DNA methylation are usually associated with imprinting-related diseases, DNA mutations, and cancer. Aberrant DNA methylation activates several repair mechanisms such as direct reversal pathway (DRR), base excision repair (BER), nucleotide excision repair and others.

In mammalian cells, human AlkB homologue 2 (hABH2) is the major housekeeping enzyme in DRR pathway. Its function is to remove a methyl group from the 1^{st} position on adenine and/or 3^{rd} position on cytosine in double- or single-stranded DNA. Such highly cytotoxic lesions are predominantly produced by internal or external alkylating agents. The occurrence of such modifications in normal, non-cancerous cells leads to the formation of the genetic mutations, followed by programmed cell death; on the other hand presence of these lesions in cancerous cells is beneficial to promote apoptosis and justifies the use of such alkylating agents as plausible and effective chemotherapeutic regimen.

Therefore inhibition of DNA repair machinery, particularly Fe(II)-dependent enzymes, like hABH2, might potentiate cytotoxic effects of the previous mentioned treatment and overcome any possible resistant mechanism that may oppose their actions. For this reason iron chelators have emerged as potential anti cancer drugs. Recently our group has shown that nitric oxide can sequester cellular iron in the form of dinitrosyliron complexes. Hence, we hypothesized that NO· could inhibit hABH2 though interaction with iron leading to inhibition of methylated DNA repair.

To test this, we have developed a novel *in vitro* method of detection for hABH2 activity. This method consists of measuring hABH2 activity on the methylated DNA followed by detection

with quantitative real-time PCR (qRT-PCR) analysis. The major advantage of this method is the ability to provide specific, robust, and accurate results and to avoid known obstacles associated with other detection methods, like radioactivity. Using this technique we have shown that nitric oxide can effectively inhibit approximately 90% of the demethylation activity of hABH2. These results have indicated that nitric oxide or nitric oxide generating compounds might be an important adjuvant therapy to the existing chemotherapeutic alkylating agents

1. INTRODUCTION

1.1 DNA methylation

1.1.1 Regulatory DNA methylation

The genetic information in the cell is encoded by DNA, which is packaged into chromatin. Epigenetic modifications are heritable chemical modifications on DNA and histones that do not alter the primary DNA sequence, but influences the expression of the underlying genes (Suzuki and Bird 2008). Examples of such changes are DNA methylation and histone deacetylation, both of which serve to suppress gene expression without altering the sequence of the silenced genes. Regulatory DNA methylation, the addition of the methyl group predominantly to a cytosine base, is an ancient evolutionary process that is associated with gene silencing, X-chromosome inactivation, and genomic imprinting (Law and Jacobsen 2010). In mammals, DNA methylation patterns are regulated by two major families of enzymes: A) DNA methyltransferase 3 (DNMT3), a family of the *de novo* methyltransferases; B) DNA methyltransferase 1 (DNMT1), a family of maintenance methyltransferase (Kim, Samaranayake et al. 2009). The DNA methylation patterns are established by the activity of DNMT3A and DNMT3B during early embryogenesis, around the time of implantation, and continue during post-implantation development for further epigenetic reprogramming in primordial germ cells. Following a wave of demethylation, a step which is required to erase DNA methylation imprints established in the previous generations, DNA methylation patterns are re-established at imprinted loci and transposable elements during gametogenesis by DNMT3A and non-catalytic paralogue, DNMT3 – like (DNMT3L). Once established, global DNA methylation patterns must be stably maintained by DNMT1 to ensure a silenced state of transposons to preserve cell type identity. DNMT1 functions primarily by restoring hemimethylated DNA state generated during

replication to a fully methylated state (Kim, Samaranayake et al. 2009). It has been shown that DNMT1 is recruited to the replication foci by an interaction with the proliferating cell nuclear antigen (PCNA) component of the replicating machinery (Law and Jacobsen 2010).

Another example of the regulatory DNA methylation is the inactivation of the X-chromosome, a process that has evolved in mammals to equalize the dosage of X-linked genes in XX females relative to XY males. Cells of early XX mammalian embryos silence randomly selected single X chromosome through hypermethylation of the CGs in the promoter region (Brockdorff 2011) and the recruitment of other transcriptional factors, like large non-coding *Xist* RNA. The resulting silenced chromosome is stable and heritable through subsequent cell divisions (Morey and Avner 2011).

In mammals, genomic imprinting results in diploid cells expressing a small subset of genes from only their maternal or paternal chromosome. Process of the genomic imprinting occurs in a stepwise manner to stably inherit correct epigenetic phenotypes. The first of these steps is an epigenator signal from outside the cell required to trigger a cellular pathway, the second is an epigenetic initiator responding to this pathway in a gene-specific manner, and the third are epigenetic maintainers that change the chromatin state at the locus recognized by the initiator and maintain this state throughout subsequent cell divisions (Barlow 2011).

1.1.2 Aberrant DNA methylation

Methylating agents can react with DNA at 12 different sites on the nucleobases, including all the exocyclic oxygens and most ring nitrogens. They can also methylate oxygen atoms in phosphates of the sugar–phosphate backbone, thereby generating methylphosphotriesters. The proportion of alkylation that occurs at different sites depends on A) the mode of chemical reaction, whether it is S_N1 or S_N2 nucleophilic substitution reaction with

the methylating agent; B) DNA state, a single- or double-stranded DNA, will determine which position will be more susceptible for the nucleophilic attack (Sedgwick 2004). Most methylating agents generate 7-methylguanine (7-meG) and 3-methyladenine (3-meA) lesions. 7-meG is usually the most abundant, since it is the most active electrophilic center for the nucleophilic attack compared to other nucleobases. S_N2 agents, in addition to above mentioned modifications, can also generate 1-methyladenine (1-meA) and 3-methylcytosine (3-meC) (Larson, Sahm et al. 1985). Examples of such reagents include methyl methanesulphonate (MMS) and the naturally occurring methyl halides, such as methyl chloride, methyl bromide, and methyl iodide. These lesions arise predominantly in single-stranded (ss) DNA or/and RNA, because in duplex DNA these reactive sites are involved in base pairing and are therefore shielded from modifications. The 7-meG lesion is relatively innocuous, whereas 3-meA, 1-meA, and 3-meC block DNA replication and are considered to be cytotoxic (Boiteux and Laval 1982). On the other hand, S_N1 agents are highly mutagenic because they react more readily with oxygens in DNA to generate mispairing adducts: A) major adduct is *O*6-meG; B) minor adduct *O*4-methylthymine (*O*4-meT). Examples of these reagents include *N*-methyl-*N*-nitrosourea and *N*-methyl-*N´*-nitro-*N*-nitrosoguanidine. The adduct *O*6-meG mispairs with thymine during DNA replication, resulting in GC→AT transition mutations. This type of mutation is considered to be a lethal lesion in human cells, possibly owing to processing of *O*6-meG containing base pairs by post-replicative mismatch repair pathway. This pathway removes mismatched bases from DNA that arise as a result of DNA replication errors by excising mispaired bases from the newly synthesized DNA strand, and refilling the gap with a correct sequence using DNA polymerases and DNA ligases (Bignami, O'Driscoll et al. 2000).

The most abundant environmental methylating agents are probably the S_N2 methyl halides, in particular methyl chloride, and S_N1 nitroso-compounds. The former is released either by biomass burning or from decaying vegetation, while the latter might be formed by the

reaction of nitrite with amines and amides in food or decaying matter. Exposure of humans to alkylating agents might come from food, cigarette smoke, occupation (these agents are used in large amounts in industrial processes) and chemotherapeutic agents (Sedgwick 2004).

1.2 DNA demethylation

1.2.1 Regulatory DNA demethylation

Although DNA methylation has been viewed as a stable epigenetic adduct, studies in the past decade have revealed that this modification is not as static as once thought. In fact, loss of DNA methylation, or DNA demethylation, has been observed in specific contexts and can occur through passive or active mechanisms. Active DNA demethylation is an enzymatic process that results in the removal of the methyl group from 5-methylcytosine (5-meC) by breaking carbon-carbon bond. By contrast, passive DNA demethylation refers to the loss of the methyl group from 5-meC when DNMT1 is inhibited or absent during successive rounds of DNA replication (Gehring, Reik et al. 2009). Genome-wide and gene-specific demethylation events have been both observed, but current evidence suggests that the former only occurs at specific times during early development, whereas the latter occurs in somatic cells responding to the specific signals. Global, genome-wide demethylation can be observed in the sperm-derived pro-nucleus within 4-8 h post-fertilization. It is observed before the completion of the first cell cycle division. Thus, it is unlikely that a passive demethylation is a contributing factor (Wu and Zhang 2010). On the other hand, validation of the passive demethylation process can be obtained from observation on the maternal genome during the developmental period, when gradual loss of DNA methylation occurs with each cell division in a replication-dependent manner. Consistent with this, maternally contributed DNMT1 is excluded from the nucleus (Monk, Boubelik et al. 1987).

Up-to-date mechanisms that describe regulatory active DNA demethylation include: A) enzymatic removal of the methyl group of 5-meC; B) base excision repair (BER), through direct excision of the 5-meC; C) deamination of 5-meC to thymine followed by BER of the T-G mismatch; D) nucleotide excision repair (NER); E) oxidative demethylation. A brief description on these mechanisms is mentioned below (Wu and Zhang 2010).

Enzymes involved in the removal of methyl group from the 5th position on cytosine are still under investigation, because only enzymes of tremendous catalytical activity would be able to catalyze this energetically unfavorable reaction. Enzymes with such capacity were reported in thymidine salvage pathway and the cholesterol synthesis pathway (Smiley, Kundracik et al. 2005).

BER DNA repair pathway involves DNA glycosylase that removes the target base resulting in an apurinic or apyrimidinic (AP) site. DNA backbone is subsequently nicked by an AP lyase to generate a 5' phosphomonoester and 3' sugar phosphate residue. An AP endonuclease then removes the 3' sugar group leaving a single nucleotide gap that is ultimately filled by DNA repair polymerase and ligase. Currently several enzymes are under investigation in this group, among them human T DNA glycosylase (Barreto, Schafer et al. 2007).

DNA demethylation can also be achieved by deamination of 5me-C to produce a thymine, followed by BER to replace the mismatched T with unmethylated C. Both cytosine deaminases and DNMTs have been proposed to carry out the first step of this mechanism. Upon deamination of 5me-C, thymine glycosylases such as TDG and methyl-CpG-binding protein 4 (MBD4) are key players in repairing the mismatch (Wu and Zhang 2010).

1.2.2 Repair of the aberrant DNA methylation

DNA damage from intrinsic and extrinsic agents causes cell death, tissue degeneration, aging, and cancer. Mammalian organism response to such damages through activation of the several repair pathways: direct reversal, base excision, and nucleotide excision. During direct reversal repair chemical bonds are broken between the nucleobase and the attached methyl group. In base excision repair, the abnormal or modified base is removed by glycosylases that hydrolyze the glycosylic bond resulting in abasic site (AP site) which is removed by AP lyase/endonucleases, and then replaced by the correct nucleotide. In nucleotide excision repair, dual incisions are made on either side of the lesion and damaged nucleotide is released in an oligomer (27-29 nt), and the resulting gap is fixed and sealed (Sancar 1995).

1.2.2.a Nucleotide excision repair

Nucleotide excision repair is a universal repair system. It can be activated for the repair of both bulky DNA adducts such as acetylaminofluorene-guanine, cisplatin-guanine, psorale N-thymine adducts, thymine dimers, and other lesions that are repaired primarily by direct repair or base excision repair. There is no known covalent base modification that is not a substrate for the nucleotide excision repair system (Huang, Hsu et al. 1994). The basic strategy of excision repair is a multi-subunit ATP-dependent nuclease (excision nuclease, excinuclease) that makes dual incisions, one on either side of the lesion, and excises oligonucleotides carrying the damage. There is some variability in the exact sites of incision depending on the lesion and the sequence context (Huang and Sancar 1994). However, as a rule of thumb, the human excinuclease removes the lesions in 24-29 mers. The excised oligomer is then replaced by DNA Polymerases and accessory factors. Human excinucleases are a family of 16 polypeptides that exist in the cell either in solitary form or in tightly held complexes. Their combined enzymatic activity results in a removal of aberrant modification on single or/and double stranded DNA.

Depending on the type of modification, certain polypeptides will be allocated and activated to execute the removal of aberrant lesions of DNA (Sancar 1995).

1.2.2.b Base excision repair

Concept of the base excision repair is the same for the regulatory DNA demethylation and repair of the aberrant DNA methylation. Enzymes that are utilized for this pathway are divided into three groups: 1st group - DNA glycosylases, 2nd group - AP endonucleases and 3rd group - Polymerases with ligases. The same AP endonucleases, polymerases and ligases are used universally in this pathway, however different DNA glycosylases depending on the type of the modification are used. Among these enzyme are Uracil-DNA glycosylase, Hydroxymethyluracil DNA glycosylase, Thymine glycol DNA glycosylase, N-methylpurine DNA glycosylase, 8-hydroxyguanine DNA glycosylase (Dodson, Michaels et al. 1994).

1.2.2 c Direct reversal repair

In humans there are two pathways of the direct reversal repair for aberrantly methylated DNA – alkyl transfer and use of dioxygenases.

Major enzyme in the alkyl transfer pathway is O6-Methylguanine-DNA Methyltransferase (MGMT). MGMT is a suicide enzyme with an active site cysteine in the sequence context of PCHRV that is conserved in all MGMTs. The enzyme repairs DNA by transferring the methyl group from O6-me-G of DNA to cysteine in an irreversible reaction resulting in the loss of the enzymatic activity. The active site of this enzyme is buried and only becomes accessible upon conformational change induced by contact with DNA. MGMT likely plays an important role in cancer prevention (Sancar 1995).

Family of the dioxygenases is represented by human homologs of the *E.coli* AlkB enzyme, second type of enzymes involved in direct reversal repair.

1.3 Eight Human homologues of the *E.coli* AlkB enzyme (hABH1-8)

In *E.coli,* AlkB was shown to repair lesions that are specifically generated by S_N2 methylating agents in ssDNA, but not in double-stranded (ds) DNA. This indicates that 1-meA and 3-meC are the sites of activity of these set of enzymes. Using protein fold-recognition method, Aravind and Koonin found that the *Escherichia coli* AlkB protein is a member of the α-ketoglutarate/Fe(II) dioxygenase superfamily. The cofactor and co-substrate requirements of AlkB were therefore suggested to be α-ketoglutarate, Fe(II) and dioxygen. They proposed that AlkB may catalyze oxidative demethylation of alkylated bases in DNA (Kurowski, Bhagwat et al. 2003). All these predictions have been proven experimentally. AlkB uses an active iron–oxo intermediate to hydroxylate 1-meA and 3-meC in DNA. The unstable hydroxymethylated intermediates decompose to yield formaldehyde, hence regenerating the unmodified base. In summary, AlkB catalyzes the direct conversion of 1-meA and 3-meC in DNA to adenine and cytosine by oxidative demethylation, which is an accurate and specific mode of DNA repair. AlkB also protects DNA against other alkylating agents and epoxides that generate hydroxyalkyl adducts. For example, 1-ethyladenine in DNA is oxidized by AlkB to regenerate adenine and release acetaldehyde. Oxidation of the larger ethyl adduct therefore occurs on carbon-1 of the alkyl group. The smallest AlkB substrate is 1-methyldeoxyadenosine 5′-monophosphate (1-medAMP), which indicates that a polynucleotide structure is not essential for efficient repair (Sedgwick 2004).

The first human protein to be described as a functional AlkB homologue was hABH1; however, this report was not supported by sufficient scientific evidence. The hABH1 cDNA did

not complement deficient repair of a damaged ssDNA phage in an alkB mutant, nor could the purified protein detectably repair 1-meA or 3-meC in assays that were carried out *in vitro*. Nevertheless, ABH1 has 18.5% identity to AlkB and could possibly have a related function (Muller, Meek et al. 2010).

hABH2 and hABH3 are two human cDNAs that do complement the *E. coli alkB* mutant phenotype. Their respective genes are located on chromosomes 12q24.1 and 11p11.2. hABH3 (also known as DEPC-1) was previously described as prostate cancer antigen-1 owing to its differential expression in prostate cancer cells. Both hABH2 and hABH3 demethylate 1-meA and 3-meC in DNA *in vitro* with the same cofactor requirements as AlkB and are therefore also α-ketoglutarate/Fe(II)-dependent dioxygenases. hABH2 is slightly more active on 1-meA, while hABH3 is more active on 3-meC in DNA (Falnes, Bjoras et al. 2004).

Based on the phylogenetic analysis supported by structure prediction and identification of characteristic conserved residues (Aravind and Koonin 2001), five more human homologues of the AlkB have been identified. hABH4, hABH5, hABH6, and hABH7 have been annotated as members of the α-ketoglutarate/Fe(II)-dependent superfamily without any details on their biological functions or possible substrates. The inabilities to purify enough quantities of these enzymes and achieve an acceptable purity of the final product are among the challenges that are faced by the biochemical characterization of these enzymes. Hence, further investigations are strongly required to decipher more features of this subgroup of enzymes (Kurowski, Bhagwat et al. 2003).

Very recently, hABH8 was found to contribute to human bladder cancer progression, indicating a possible role of AlkB homologues in cancer development (Chen, Liu et al. 2010).

1.4 Human AlkB homologue 2 (hABH2)

The human AlkB homologue 2 (hABH2) is a housekeeping enzyme that primarily repairs methyl and ethyl lesions on adenine and or cytosine in mammalian dsDNA. hABH2 is a relatively small basic protein with 200–400 amino acids (Ringvoll, Moen et al. 2008). A sequence alignment has shown that the three residues: His 131, Asp 133 and His 187 constitute the iron-binding domain which is conserved in all other members of hABH family. On the basis of comparisons with other well-characterized α-ketoglutarate/Fe(II)-dependent dioxygenases, the Arg 204, at the start of a conserved cluster of amino acids, is likely to be involved in binding of C5 carboxylate of α-ketoglutarate (Aas, Otterlei et al. 2003). hABH2 has developed several structural features that are distinguishable from other members of the hABH family and add to its unique substrate recognition machinery. hABH2 has specific binding motifs in the form of positively charged RKK loops that assist in binding the complementary strand of DNA. It also has a crucial hairpin motif that bears the finger residue Phe 102. This intercalating residue fills the void created by the flipped 1-meA and maintains the normal length and stacking of duplex DNA. These described structural characteristics are responsible for the ability of hABH2 to operate on dsDNA in a sequence independent manner (Chen, Liu et al. 2010). Even though, it has been detected that hABH2 effectively removes alkyl group from both 3-cytosine and 1-adenine, approximately 4-fold preference towards 1-meA is present (Mishina and He 2006). As for the localization, mRNA of hABH2 at variable levels was clearly detected in 10 different human tissues and several different cell lines derived from carcinomas by Northern hybridization. Relatively high levels of hABH2 mRNA were present in liver and bladder. In cell lines derived from carcinomas, relatively high presence of mRNA was detected in HeLa, cervical cancer cell lines. hABH2 is localized in cell nuclei, where it is diffused throughout the nucleoplasm and accumulated in nucleoli. hABH2 is not found in mitochondria as a repair enzyme, as it has not been shown to punctuate cytoplasmic staining typical of mitochondrial proteins (Duncan, Trewick et al. 2002).

1.5 Historical input of nitric oxide research

The free radical nitric oxide (NO·) is the best example of a reactive molecule demonstrating both cytotoxic and cytoprotective properties. NO· was identified in the 1980s as an endothelium-derived relaxation factor and the active component of nitrovasodilators capable of causing vascular relaxation. Additionally, NO· was found to be generated by macrophages participating in the antitumor and anti-pathogen response. These few initial observations potentiated a new field of investigation and led to an extensive exploration of NO· importance, in almost every tissue in the body. However, contradictory results began to emerge concerning the participation of NO· in pathophysiological responses (Ignarro 1996). Whereas a number of studies implied the cytotoxic nature of endogenous NO·, others showed a protective effect of NO·. It was shown that the NO·-mediated toxicity can be attributed to the generation of reactive nitrogen oxide species capable of causing cell death, whereas the protective effects have been proposed to be through antioxidant mechanisms. Over the past couple of decades, there was an extensive debate on the exact mechanism of this dichotomy and whether NO· is possessing a deleterious or a beneficial effect (Thomas, Ridnour et al. 2008).

1.6 Biological implication of nitric oxide

Nitric Oxide (NO·) is an ubiquitous free radical signaling molecule that regulates many cellular processes including angiogenesis, smooth muscle tone, immune response, apoptosis, and synaptic communication (Hickok and Thomas 2010). Paradoxically, NO· had been implicated as a promoter of the severity of different diseases, including cancer and stroke. In fact, both protective and deleterious properties were assigned to NO· even in context of the same physiological event. Unlike most other biological mediators, the *in vivo* properties of NO·

are determined by its chemistry. Nitric oxide can undergo numerous reactions and these can often result in the formation of the reactive nitrogen oxide species (RNOS).

Chemical reactions of NO· can be classified into two categories: direct and indirect reactions. Direct chemical reactions are those in which NO· directly interacts with the biological targets. The most common reactions of this type are between NO· and heme-containing proteins. These reactions are rapid and represent the majority of the *in vivo* effects of NO·. On the other hand, indirect effects involve other RNOS, usually derived from the reaction of NO· with O_2 or superoxide (O^{2-}). Indirect effects demand much higher concentrations of NO· than direct reactions. Therefore, NO· produced at low concentrations for short periods of time will result in direct effects, while indirect effects will occur in regions where higher NO· concentrations are maintained for a longer time (Wink and Mitchell 1998).

The initial investigation on NO· biological effects focused on chemical and biochemical modifications of different biological targets. As the understanding of the molecular biology of NO·, its related targets, and the physiological framework of NO· generation expanded, it became evident that the ability of NO· to elicit a specific biological responses was highly dependent on its concentration. Variety of proteins that are known to be post-translationally modified in response to NO· has been assessed to determine if the redox chemistry differentiates those responses (Thomas, Ridnour et al. 2006). For instance, when breast cancer cell lines were exposed to NO· at various concentrations for defined periods of time, various proteins were found to be sensitive to different concentrations of NO·. At sustained NO· levels between 10 and 30 nM, phosphorylation of ERK occurs through a cGMP-dependent mechanism. At 30–60 nM NO· Akt is phosphorylated. When NO· reaches a threshold concentration of about 100 nM, HIF-1α is stabilized. At 400 nM NO·, p53 is phosphorylated and acetylated. It is only above 1 mM NO· that nitrosation of critical proteins such as PARP, caspase, and others occurs. In the Petri dish, this upper level is where NO· inhibits

mitochondrial respiration. The results of these and other studies provided insights regarding specific mechanisms of action of NO· as well as highlighting its dichotomous nature under various biological conditions. This has suggested that NO· responses are highly organized and concentration dependent. The first level of signaling is cGMP dependent, where low doses (< 1–30 nM) of NO· can mediate proliferative and protective effects. As NO· levels increase, Akt becomes phosphorylated at serine 472, an event known to be protective against apoptosis by inducing the phosphorylation of Bad and caspase-6. At higher NO· concentrations HIF-1α is stabilized leading to a proliferative response which is important to mediate protection against tissue injury. When NO· levels are sufficiently high to induce p53 phosphorylation, a cytostatic and even apoptotic response is elicited. As a general rule, it was concluded that relatively low concentrations of NO· favor pro-growth and anti-apoptotic responses, whereas higher levels of NO· favor pathways that induce cell-cycle arrest, aging, or apoptosis (Thomas, Ridnour et al. 2008).

1.7 Chemical reaction of nitric oxide with metals

Unique physical and chemical properties of nitric oxide dictate that under biological conditions it reacts with only a minority of chemical species, i.e., other radicals and transition metals. Coordination of NO· to iron heme-proteins, is an important aspect of its physiological utility. In fact, NO· is an extremely good ligand for ferrous hemes, and unlike other simple diatomic ligands, such as O_2 and CO, binds ferric heme as well (although the affinity of NO· to ferrous heme is significantly greater). One of the most important function of biological NO· is to serve as an activator of the iron heme-containing enzyme guanylate cyclase (Fukuto *et al.*, 2000). Another example of NO· inhibition of a heme enzyme is in the respiration chain. Nitric oxide forms a nitrosyl with the heme of cytochrome aa3 in complex IV of mitochondria thus

inhibiting oxygen reduction. Under normal physiological conditions, most cells require μM concentrations of NO· levels to inhibit mitochondria, but such level of NO· is only possible during immune response. Under lower O_2 tension associated with a rapid respiration rate, such as in the heart muscle, considerably lower NO· levels are required to inhibit respiration. This highlights the importance of the biological interactions of NO· and its metabolism (Flores-Santana, Switzer et al. 2009).

Formation of metal-nitrosyls in biological systems can give rise to several paramagnetic species, which can be observed by EPR spectroscopy, and has been utilized to glean important information regarding the biological actions of NO·. In particular, exposure of cells or tissues to NO· (either exogenously administered or endogenously synthesized) results in the ubiquitous appearance of a “g (paramagnetic value) = 2.04” axial EPR signal, which has been assigned to iron in square planar coordination with two nitrosyl ligands, denoted “dinitrosyliron complexes” (DNIC) (Toledo, Bosworth et al. 2008). Within the cells, such reservoir of iron is mostly coming from chelatable iron pool (CIP). This small methodologically defined population of redox-active iron is associated with a diverse population of both high- and low-molecular-weight cytosolic ligands. After formation, DNIC possess NO-mimetic properties with regard to guanylyl cyclase activity and phenotypic responses. Quantitatively, they represent the largest intracellular pool of NO-derived cellular adducts and are more physiologically important than previously realized (Hickok, Sahni et al. 2011).

Nitric oxide as a free radical signaling molecule participates in a wide variety of biologically relevant processes. Since spectrum of its activity is so broad, extensive investigations should be performed in order to understand capacity of this molecule for potential therapeutic applications. One of the emerging areas of nitric oxide research is its chemical reactions with transient metals, like iron in the form of heme-bound proteins, chelatable iron pool or non-heme iron-dependent enzymes. That’s where the initial interest of the present research

lies. Since it is a well established fact that NO· forms stably enough complexes with iron, we investigated its inhibitory effect on the member of α-ketoglutarate/Fe(II)-dependent family of enzymes – hABH2. As mentioned previously, the biological significance of this dioxygenase is in its ability to repair cytotoxic lesions of DNA nucleobases. During anticancer treatment such kind of lesions are usually introduced by alkylating compounds to prevent replication and division of neoplasias. That's why use of nitric oxide to inhibit hABH2 can be of great importance as an adjuvant anticancer therapy to enhance cytotoxic effects of currently used drugs and overcome any potential resistance mechanism.

For determination of nitric oxide effects on hABH2, a novel detection method has been developed in our lab. We linked quantitative real-time PCR analysis to the hABH2 activity assay that was previously established. With such means of detection, we observed approximately 90% inhibition of hABH2 activity with 100 μM spermine NONOate – Sper/NO treatments. The results and devolved methods shown in this research serve as a preliminary proof of the original hypothesis, enabling further investigations of NO· effects on hABH2 itself and other members of α-ketoglutarate/Fe(II)-dependent family of enzymes at the cellular level.

2. MATERIALS AND METHODS

2.1 Materials

Caution: All treatments with alkylating agent: methyl methanesulfonate were handled in accordance with Hazard and Precautionary Statements. All chemicals were purchased from Life Technologies (Grand Island, NY), Fisher Scientific (Itasca, IL) or Sigma-Aldrich (St.Louis, MO) unless stated otherwise. Agarose, molecular biology grade, was purchased from ISC BIOEXPRESS. Kits for polymerase chain reactions (PCR, qRT-PCR) were purchased from BioRAD (Hercules, CA), Promega (Madison, WI) or Applied Biosystems (Carlsbad, CA). Primers were ordered from Life Technologies (Grand Island, NY). Histone Demethylase Fluorescent Activity Kit was a generous gift from Arbor Assay (Ann Arbor, MI). Recombinant hABH2 enzyme was purchased from Abcam (Cambridge, MA). QIAEX II gel extraction kit was purchased from Qiagen (Valencia, CA). DpnII restriction enzyme and Taq DNA polymerase were purchased from New England Biolabs (Ipswich, MA). Synthetically prepared DNA with single 3-methyl cytosine incorporation was purchased from GeneLink (Hawthorne, NY). Cell lines (HCC 1806, MDA-MB-231), used for DNA extraction were purchased from ATCC (Manassas, VA). Spermine NONOate (Sper/NO) was a generous gift of Dr. Joseph Hrabie (National Institute of Health, NCI)

2.2 Methods

2.2.1 Genomic DNA extraction

Genomic DNA extraction consisted of 2 parts: cell lysis and DNA extraction.

2.2.1.a Cell lysis

HCC 1806 and/or MDA-MB-231 cancer cell lines were grown in supplemented with 10% FBS and 1% P/S RPMI-1640 or DMEM medium, respectively, until 70% confluence. Cells were washed twice with warm PBS and trypsinized with 7 mL of trypsin. After trypsinization cells were centrifuged for 10 min at 1500 rpm in the bench-top centrifuge. Supernatant was removed and cell pallet was flesh frozen in dry ice/ethanol bath. Pallet was thawed, divided equally between 4 tubes and re-suspended in 1 mL sucrose lysis solution (50 mM Tris/HCl (pH 8.0), 40 mM EDTA (pH 8.0), 0.75 M sucrose, nuclease-free water). Cells were vortexed for 5 min intervals for 30 min and centrifuged for 30 min at 3500 rpm at 4 °C. 750 µL of supernatant were removed and pallet was re-suspended in 250 µL of the left-over supernatant. 1mL of the re-suspension buffer (150 mM NaCl, 10 mM EDTA, 50 mM Tris/HCl (pH 8.0)), was added to each tube and cells were centrifuged for 30 min at 3500 rpm at 4 °C.

2.2.1.b DNA Extraction

After centrifugation, all supernatant but 100 µL was removed. 12.5 µL of 10X TEN solution, 6.25 µL of 2 mg/ml proteinase K, and 12.5 µL of 10% SDS were added. Tubes were incubated at 37 °C overnight in order to increase yield of proteins and lipids digestion. 150 µL of phenol: chloroform: isoamyl alcohol mixture (25:24:1) were added and mixed by vortexing. Tubes were centrifuged for 15 min at 1500 rpm. After centrifugation organic phase from the bottom of the tube was removed and washes with phenol: chloroform: isoamyl alcohol mixture were repeated until white protein layer at the interface did not disappear. Aqueous layer was transferred to a fresh tube and extracted twice with equal volume of chloroform as mentioned above. Aqueous layer was again transferred to a fresh tube and precipitation buffer (0.1 volumes 3 M CH_3COONa, 2 volumes ice-cold isopropanol (molecular biology grade) and 0.01

volumes of linear polyacrilamide) was added to it. Tubes were incubated at -80 °C overnight to enhance precipitation of DNA. After precipitation tubes were centrifuged at 13000 rpm for 30 min at 4 °C. Supernatant was removed and double volume of 70% ethanol was added, which proceeded with centrifugation at 13000 rpm for 10 min at 4 °C. Supernatant was removed and pallet was air-dried for 30 min or until no traces of alcohol were detected. DNA was re-suspended in appropriate amount of 10 mM Tris/HCl (pH 8.0). Concentration of DNA was determined by NanoDrop 1000 Spectrophotometer.

2.2.2 Agarose gel electrophoresis

Agarose gel electrophoresis has been performed on Sub-Cell GT Agarose Gel Electrophoresis System (BioRAD, Catalog# 170-4401). Gels were individually casted with 2% agarose in them. 1.5 g of molecular grade agarose was added to 75 mL of 1X TAE buffer (Tris Base/Glacial Acetic acid/EDTA). Agarose dissolving requires micro waiving for 30 sec intervals until no residual particles can be seen in the solution and it becomes clear. After agarose cooled down to approximately 60 °C, ethidium bromide 0.5 µg/ml was added. Agarose with ethidium bromide was poured on the casting membrane for solidification. DNA product from PCR analysis, previously mixed with loading dye (0.4% orange G, 0.03% bromophenol blue, 0.03% xylene cyanol FF, 15% Ficoll® 400, 10 mM Tris-HCl (pH 7.5) and 50 mM EDTA (pH 8.0)), was added to the wells on the gel. After addition of DNA sample, container was filled with running buffer (1X TAE (Tris Base/Glacial Acetic acid/EDTA)), sealed and connected to the power supply. Electrophoresis was done on 100 V for approximately 1 h.

2.2.3 Methylation of the genomic DNA

In order to achieve methylation of the genomic DNA, alkylating agent – methyl methanesulfonate (MMS) was used. Previously extracted DNA was equally divided between two vials and MMS (2 mM) was directly added to the tube for 15 min. One vial was kept in 95 °C for the duration of the reaction, to achieve denaturation of double stranded DNA. Another vial was kept at a room temperature to maintain a non-denatured state of DNA. After 10 min, reaction was quenched for 20 min on ice. Methylated DNA was directly used for the enzyme assay.

2.2.4 hABH2 activity fluorescence detection method

A fluorescence activity kit (Arbor Assay, Catalog# K010-F1) has been used to directly detect the activity of hABH2. The detection method is based on the measurement of the fluorescence signal generated by a side product of hABH2 catalyzed reaction - formaldehyde. Reaction was set up as following: 50 µL of 2 mM ascorbate, 100 µM $FeSO_4$ and 25 µL of either formaldehyde standards, hABH2 enzyme or a blank, all prepared in provided kit buffers, followed by 25 µL of methylated DNA containing 2 mM α-ketoglutarate, also dissolved in the provided kit buffers. After addition of all components, plate was sealed and incubated at 37 °C for 2 h. To quench the reaction, 5 µL of 4 mM deferoxamine, an iron chelator, dissolved in the assay buffer has been used. 25 µL of the fluorescence developing reagent was then added to each well and incubated at 37 °C for 30 min. After incubation, plate was read on Synergy H4 Hybrid Multi-Mode Microplate Reader (BioTeck, Winooski, VT) with excitation at 450 nm and emission at 510 nm wavelength, respectively.

2.2.5 DNA extraction after electrophoresis

For extraction of DNA from agarose gel after electrophoresis, QIAEX II® Gel Extraction Kit has been used (QIAGEN, Catalog# 20021). Extraction was done as following: bands corresponding to the correct DNA fragments were removed from the gel using a clean and sharp scalpel. The samples were placed into 1.7 mL eppendorf tube and weighted. 3 volumes of the washing buffer QX1 and 20 µL of binding suspension QIAEXII were added. Tubes were incubated at 50 °C for 10 min to solubilize the agarose and bind the DNA. The mixture was vortexed every 2 min to keep QIAEX II in the suspension and then followed by centrifugation for 30 sec and careful removal of supernatant. Pallet was washed with 500 µL of buffer QX1 for the second time, after which it was washed twice with 500 µL of the PE buffer. After second wash pallet was air-dried for approximately 30 min or until it turned white. To elute DNA, 20 µL of 10 mM Tris/HCl (pH 8.0) was used to re-suspend the pallet. The resulting mixture was incubated for 5 min on the bench-top. Tubes were centrifuged for 30 sec at 15000 rpm at 4 °C and supernatant was carefully removed to a clean vial. To increase yields of DNA, a second re-suspension with 10mM Tris/HCl (pH 8.0) was done, as described previously. DNA concentration was checked on NanoDrop 1000 Spectrophotometer.

2.2.6 Restriction digest of the DNA

Restriction digest was performed on the PCR product of the genomic DNA to validate experimental set-up. Genomic DNA was extracted from cancer cell lines: HCC 1806 and/or MDA-MB-231 as previously described. PCR product was achieved by selective amplification of the specific region in the genomic DNA containing 5'-GATC-3' sequence. For the amplification, part of the C-MYC exon was selected. The primers (Life Technologies) used for this reaction were designed such that forward and reverse primers will be complementary to 20 first base-pairs on the sequence. Primers used for amplification were:

Forward primer: 5' - TGTGCGTAAGGAAAAGTAAG – 3'

Reverse primer: 5' – TCTTTCAGTCTCAAGACTCA – 3'

Primers were reconstituted in nuclease free water to a final concentration of 90 µM. A typical PCR reaction was run with Promega GoTaq Flexi DNA Polymerase Kit (Catalog #M8291) in 50 µL, containing 10 µL of 5X Colorless GoTaq Flexi Buffer, 2 mM $MgCl_2$, 0.2 mM each dNTP, 200 nM each primer, 1.25 U GoTaq DNA polymerase, 0.5 µg of the genomic DNA and nuclease free water to 50 µL. The PCR cycling conditions were: 95 °C (10 min), 95 °C (45 sec), 53 °C (1 min), 72 C (45 sec)] x 35 cycles, 72 °C (4 min). The PCR products from several reactions were combined and subjected for agarose gel electrophoresis, for visualization of the results. Bands corresponding to the correct product were excised from the gel and DNA was extracted using QIAEX II gel extraction kit (QIAGEN, Catalog# 20021) by method mentioned before. After elution, DNA concentration was checked on NanoDrop Spectrophotometer and the eluent proceeded to the precipitation. Precipitation buffer was calculated based on the volumes of the eluted DNA. Major components of the buffer were: 0.1 volume 3M CH_3COONa, 0.01 volume linear polyacrilamide and 3 volumes of isopropanol (molecular grade purity). Overnight precipitation at -80 °C was followed by reconstitution of DNA in 10 mM Tris/HCl (pH 8.0) solution. Final concentration of DNA was determined by NanoDrop 1000 Spectrophotometer.

DpnII restriction digest (New England Biolabs, Catalog# R0543T) was run in a total volume of 20 µL containing: 20 U of DpnII enzyme, 1X NEBuffer DpnII, 500 ng of the PCR product. Reaction was carried out at 37 °C for overnight. Digestion was followed with heat inactivation of DpnII enzyme at 65 °C for 20 min and overnight precipitation at -80 °C, using previously mentioned components of the precipitation buffer. Results of the digestion were visualized by running PCR reaction. As DpnII cleaves oligonucleotide into 2 pieces, we constructed specific primers that were able to amplify both cleaved part. Primers amplifying

intact oligonucleotides were labeled “long”; since forward primer for cleaved and intact oligonucleotides were the same, only reverse primer was constructed for the cleaved oligonucleotides, which we labeled as “short”. Primers used for amplification were:

Forward primer long: 5’ - TGTGCGTAAGGAAAAGTAAG – 3’

Reverse primer long: 5’ – TCTTTCAGTCTCAAGACTCA – 3’

Reverse primer short: 5’ – ATGCATTTGAAACAAGTTCA – 3’

PCR amplification of the restriction digest product was carried out using previously mentioned conditions and cycling parameters. Results of the PCR analysis were visualized using agarose gel electrophoresis, as described previously.

2.2.7 hABH2 activity assay

hABH2 activity assay was carried out in 50 µL reaction using 63.6 nM (100 ng) of the recombinant enzyme (Abcam, Catalog # ab105622), 50 mM Tris/HCl (pH 8.0), 2 mM ascorbate, 100 µM α-ketoglutarate, 40 µM $FeSO_4$, 10 mM $MgCl_2$, and 49.5 nM (200 ng) of the synthetically prepared DNA with one 3-methyl cytosine incorporation (GeneLink,). Sequence of the DNA was:

5’-TGTGCGTAAGGAAAAGTAAGGAAAACGATTCCTTCTAACAGAAATGTCCTGAGCAATC
ACCTATGAACTTGTTTCAAATGCATGAT[3-methyl-dC]AAATGCAACCTCACAACCTTGGCTG
AGTCTTGAGACTGAAAGA-3’

Reaction was carried out at 37 °C for 30 min and quenched by heat-inactivation of the enzyme at 60 °C for 20 min. The homogenous solution was subjected for DNA precipitation using the same precipitation protocol, as mentioned previously. Vials were kept in -80 °C

overnight. DNA was reconstituted in 10 mM Tris/HCl (pH 8.0). Final concentration of DNA was determined by NanoDrop 1000 Spectrophotometer.

The function of the enzyme was evaluated using quantitative real-time PCR analysis (qRT-PCR). Reactions were carried out in 96-well plate with a total volume of 20 µL. Components of the reaction were: 10 µL 2x Fast SYBR® Green Master Mix (Applied Biosystems, Catalog # 4385610), 200 nM of reverse and forward primers and 1 ng of DNA. Primers for qRT-PCR were designed as described before:

Forward primer: 5'-TGTGCGTAAGGAAAAGTAAG-3'

Reverse primer: 5'-TCTTTCAGTCTCAAGACTCA-3'

Analysis was carried out on Applied Biosystems StepOnePlus™ quantitative real-time PCR cycler. PCR cycling conditions were: 95 °C (10 min), [95 °C (30 sec), 53 °C (1 min)] x 40.

2.2.8 hABH2 treatment with nitric oxide

To assess the effects of nitric oxide on hABH2, enzyme was treated with 100 µM spermine NONOate – Sper/NO. Reactions were designed as previously described (all required co-factors were added, also duration and temperature of the reaction were kept as before) with few modifications. hABH2 was pre-treated for 10 min with either 100 µM Sper/NO before adding DNA with one 3-methyl cytosine incorporation to the reaction. After addition of DNA and nuclease free water, assay proceeded as previously described.

3. RESULTS

3.1 hABH2 enzymatic activity

In the present study, our major goal was to elucidate the effects of the free radical nitric oxide on the Fe(II) – dependent enzyme – hABH2. Based on the hypothesis stated previously, our goal was to measure changes in the enzymatic activity of hABH2 after nitric oxide treatment. In order to proceed with such measurements we set up to develop a novel detection method for hABH2 activity, since the only currently available technique has a lot of disadvantages that we wanted to avoid (i.e. radioactively labeled DNA).

3.2 Methyl methanesulfonate alkylation of the genomic DNA

As has been previously shown (Wyatt and Pittman 2006) that methyl methanesulfonate (MMS) is a strong alkylating agent. The position on the nucleobase, at which the alkylating attack will happen, directly depends on its nucleophilicity. This is partially determined by the state of the DNA itself, whether it is single-stranded or double-stranded. We were mostly interested in two positions: *N*1-adenine and *N*3-cytosine, since they are hot spots for hABH2 activity. *N*1-adenine and *N*3-cytosine are much more reactive as nucleophiles in the absence of hydrogen-bonding participation, that is, these two sites are much more susceptible to methylation in single stranded DNA (Wyatt and Pittman 2006).

Keeping this in mind we methylated genomic DNA that was previously extracted from cancer cells (MDA-MD-231 and/or HCC 1806), in two ways in order to achieve better yields of the alkylation. During the reaction the first tube of genomic DNA was kept at room temperature, to maintain its double-stranded state and a second tube was kept at 95 °C, to achieve denaturation of DNA and maintain it in a single-stranded state. Alkylating agent – MMS (2 mM) was directly added to DNA for 15 min followed by quenching for 20 min on ice. Detection of hABH2 activity was done by means of agarose gel electrophoresis. We thought that regular

non-methylated DNA methylated DNA and methylated DNA after hABH2 assay will demonstrate different shifting patterns on the agarose gel. Before proceeding to the hABH2 assay we validated the detection technique by running regular non-methylated DNA, non-denatured methylated DNA and denatured methylated DNA on the agarose gel. This set-up was supposed to show us which state of DNA we should maintain in order to achieve proper methylation levels. As you can see from **Figure 1**, denatured methylated DNA didn't give us a solid band indicating either complete degradation of DNA molecule itself, potentially due to the harsh conditions of the methylation reaction, or extensive methylation of nucleobases at the positions preventing re-annealing of the DNA, so that ethidium bromide is unable to detect double-stranded DNA. As well, no difference in terms of visual representation of the bands, or their speed of shifting on the agarose gel during electrophoresis, was detected between non-methylated regular DNA and non-denatured methylated DNA.

Because this method did not provide reliable results we decided to terminate use of this method in future experiments for detection of hABH2 activity and proceed with a fluorescence based detection method.

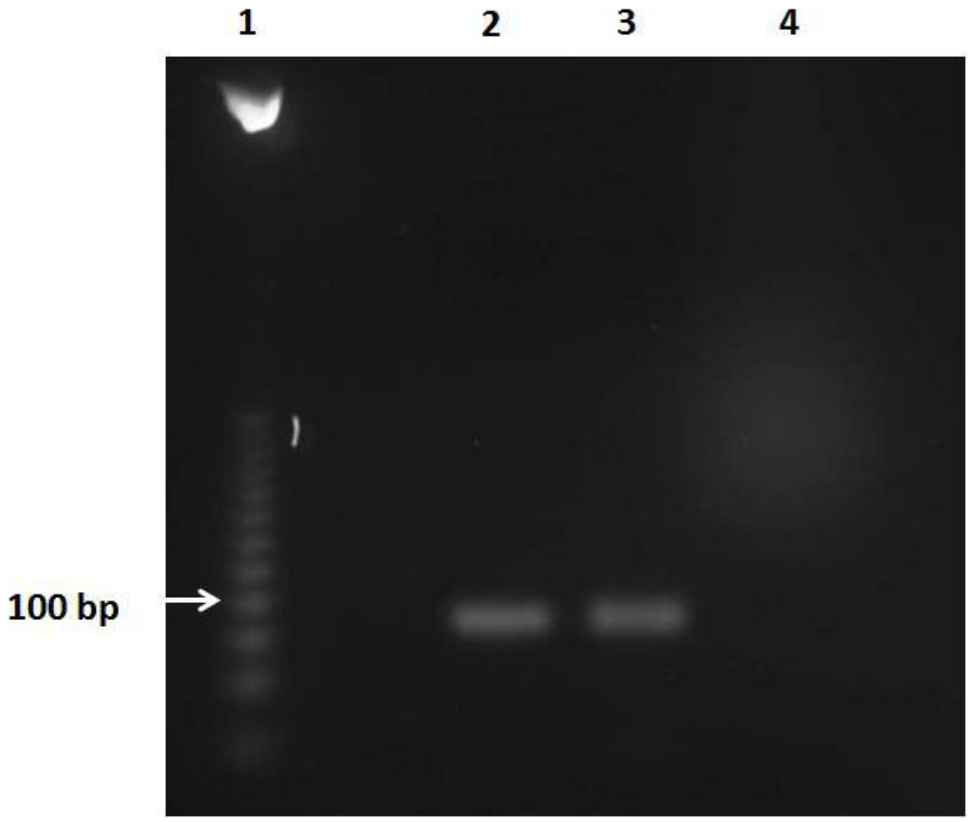

Figure 1: Results of the agarose gel electrophoresis of methylated DNA. 3 DNA samples were run on 2% agarose gel. 1) 25 bp DNA step ladder, 2) regular non-methylated DNA, 3) non-denatured methylated DNA, 4) denatured methylated DNA.

3.3 Fluorescence based method of hABH2 activity detection

While looking for other methods of detection for hABH2 activity we found a fluorescence activity kit (Arbor Assays, Catalog # K010-F1) that was validated for the detection of another Fe (II)-dependent enzyme activity – *Jumonji*-type demethylase. Components of the kit are designed in such a manner, that they detect fluorescence signal from a side product of the enzyme demethylation reaction – formaldehyde. Since the side product of hABH2 reaction is the same, we chose this method as another step in elucidation of the correct detection method for hABH2.

As an initial validation step we ran an experiment to confirm proper substrate for hABH2, either non-denatured methylated DNA or denatured methylated DNA, since results from

previous experimental method were inconclusive. Substrate - methylated DNA was freshly prepared as previously described. Assay was prepared as indicated previously.

As you can see from **Figure 2** our initial experiment showed that denatured methylated DNA is more favorable substrate for hABH2 then non-denatured methylated DNA.

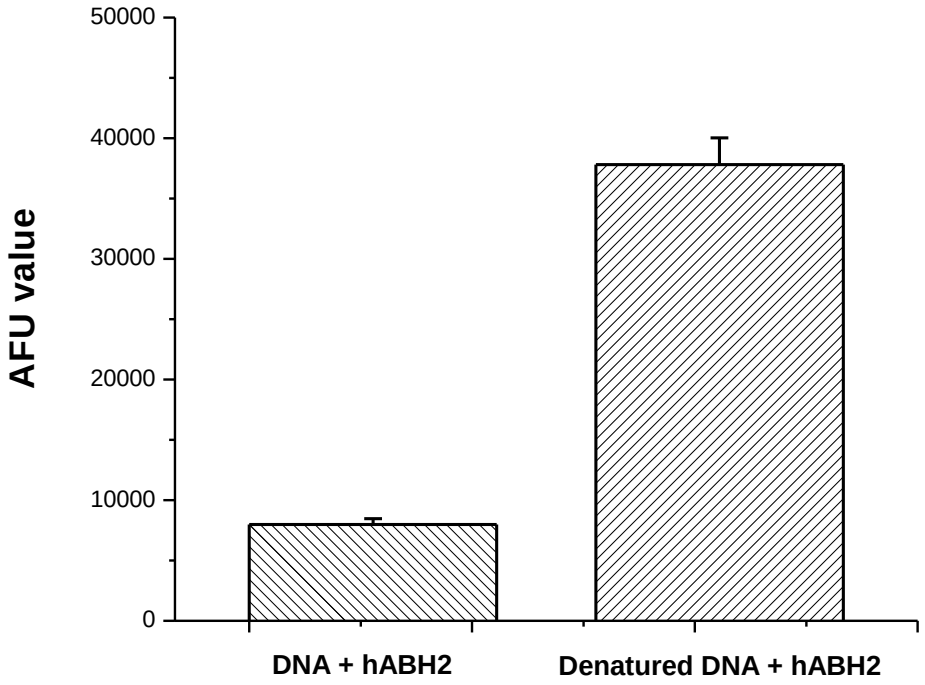

Figure 2: Initial validation of the substrate for hABH2. DNA + hABH2 – DNA from the hABH2 assay with methylated non-denatured DNA; Denatured DNA + hABH2 – DNA from the hABH2 assay with methylated denatured DNA. AFU – arbitrary fluorescence unit.

Based on these results, we selected denatured methylated DNA as a substrate for hABH2. Our next step was to achieve proper negative controls and to distinguish differences in the fluorescence signal between non-methylated DNA, denatured methylated and denatured methylated DNA from hABH2 assay. As it can be seen from **Figure 3** that the goals set for this experiment were not achieved, since fluorescence signal from non-methylated DNA is the highest. Even though the florescence detected from DNA after hABH2 assay is higher than its

negative control – denatured methylated DNA, results are still inconclusive. Potentially this kit is not suitable for the detection of DNA demethylases activity such as hABH2.

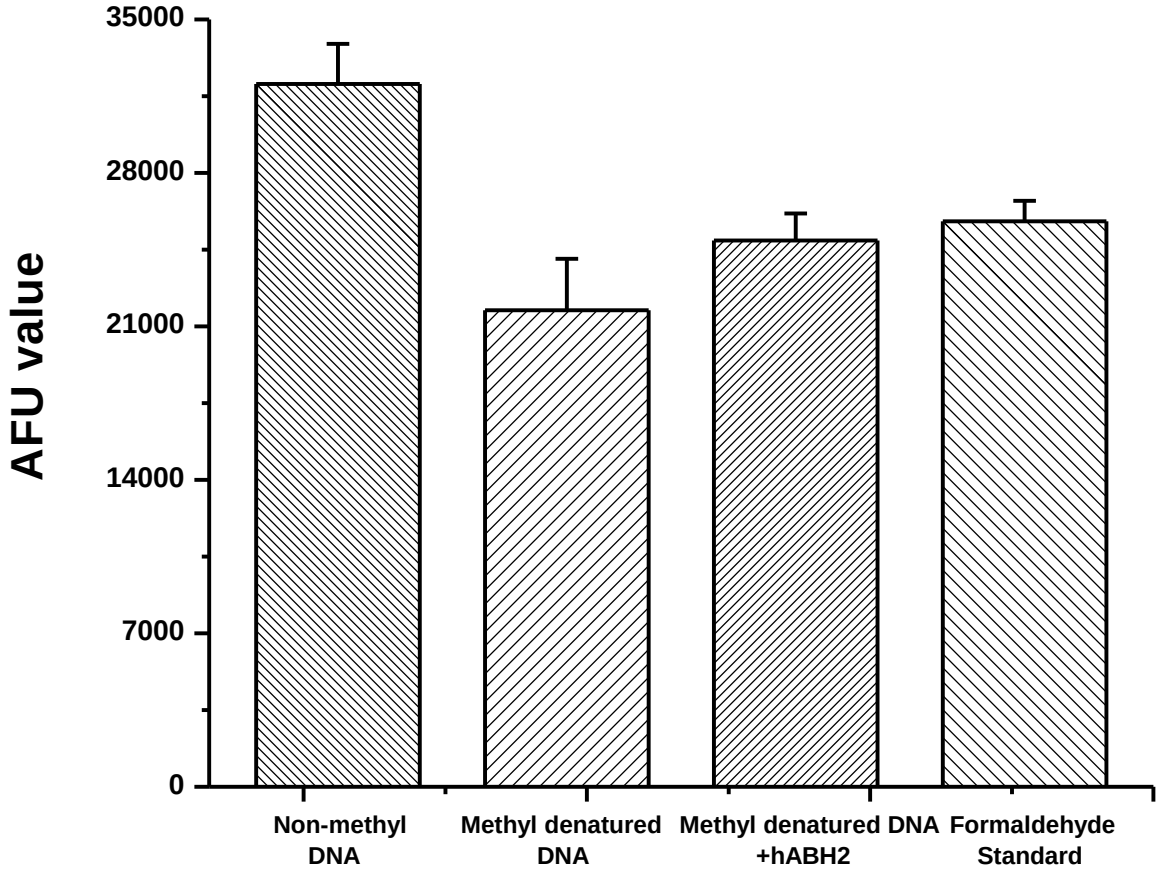

Figure 3: Determination of the negative controls for hABH2 assay. Non-methyl DNA – non-methylated DNA; Methyl denatured DNA – denatured methylated DNA; Methyl denatured DNA+hABH2 – DNA sample from hABH2 assay with methylated denatured DNA; Formaldehyde standard – solution of formaldehyde (100 µM); AFU – arbitrary fluorescence unit.

3.4 DpnII restriction digest as an hABH2 activity detection method

DpnII is a methylation sensitive restriction enzyme. It works on DNA oligonucleotides, containing 5'-GATC-3' recognition sequence. A unique feature of this enzyme – is that its activity is blocked if either adenine or cytosine on the recognition sequence is methylated. Using

this characteristic of the enzyme, we specifically amplified by means of the PCR analysis a genomic sequence that had DpnII recognition site:

5'-TGTGCGTAAGGAAAAGTAAGGAAAACGATTCCTTCTAACAGAAATGTCCTGAGCA

ATCACCTATGAACTTGTTTCAAATGCAT**GATC**AAATGCAACCTCACAACCTTGGCTGAGTCT

TGAGACTGAAAGA-3'

Primers and cycling conditions were as previously described. After amplification, PCR products were purified by running on agarose gel and consecutively extracted from it. After purification DNA was directly used for DpnII digest. Reaction was set up as previously described. Digest was run in 37 °C for 1 h. In order to achieve better quality of the DNA yields after DpnII digest proper reaction quenching method had to be established. We determined two mechanism of inactivation. First one was heat inactivation for 20 min at 65 °C right after the digest and the second was DNA precipitation overnight at -80 °C. After quenching the reaction, 3 samples were subjected for PCR analysis – non-digested DNA as a control, digested DNA from heat-inactivated sample and digested DNA from precipitated sample.

PCR set-up and cycling conditions were as previously described with one modification – special design of the primers. Since DpnII cuts DNA oligonucleotides into two parts, we constructed primers for this PCR amplification in the way as it is shown in **Figure 4**. Primer 1 (P 1) and primer 2 (P 2) amplify cut copies of the oligonucleotide and primer 1 and primer 3 (P 3) amplify un-cut copies of the oligonucleotide. Results of PCR amplification were visualized by means of agarose gel electrophoresis.

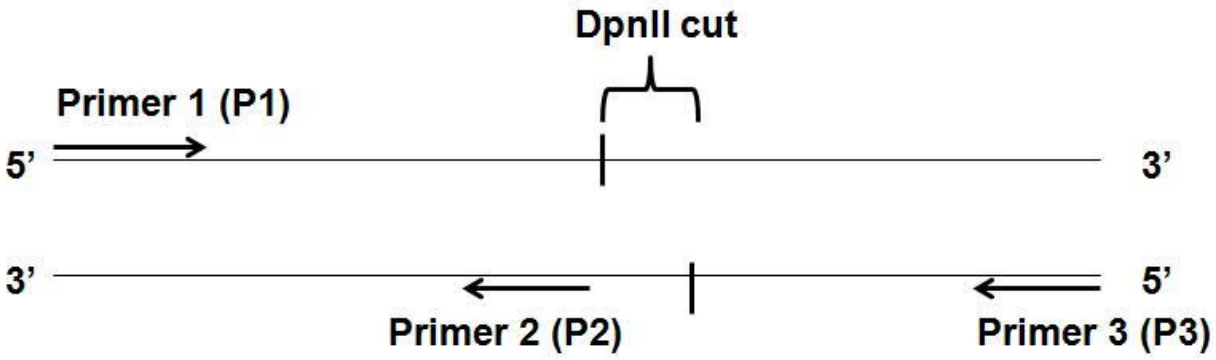

Figure 4: Schematic overview of primers construction for PCR amplification after DpnII digest. Primer 1 – starts amplification of cut/un-cut oligonucleotides from 5' direction. Primer 2 – starts amplification of cut oligonucleotides from 3' direction. Primer 3 – starts amplification of the complementary strand of the un-cut oligonucleotides from 5' direction.

Figure 5 shows that heat-inactivation is not the most effective method of quenching DpnII digest, though faint bands corresponding to the products with correct molecular weight are still present. Precipitated sample, on the other hand, based on the visual representation of the restriction digest seems to be a better approach for quenching DpnII digest. Major discrepancy observed on the gel is that digest didn't go all the way through and amplification of the un-cut oligonucleotides (bands corresponding to the PCR product with higher molecular weight) still can be seen. Based on the obtained results we decided to quench DpnII digest by a combination of both methods – heat inactivation for 20 min at 65°C and precipitation of DNA in -80 °C overnight in order to summarize their positive effects to achieve better quality of the DNA product.

Results, represented on the agarose gel (**Figure 5**) showed us that PCR amplification needs further improvements as well. Changes added to the PCR process were as following:

1) Extension time on the PCR cycler was prolonged to 1 min;

2) Number of cycles was increased up to 40.

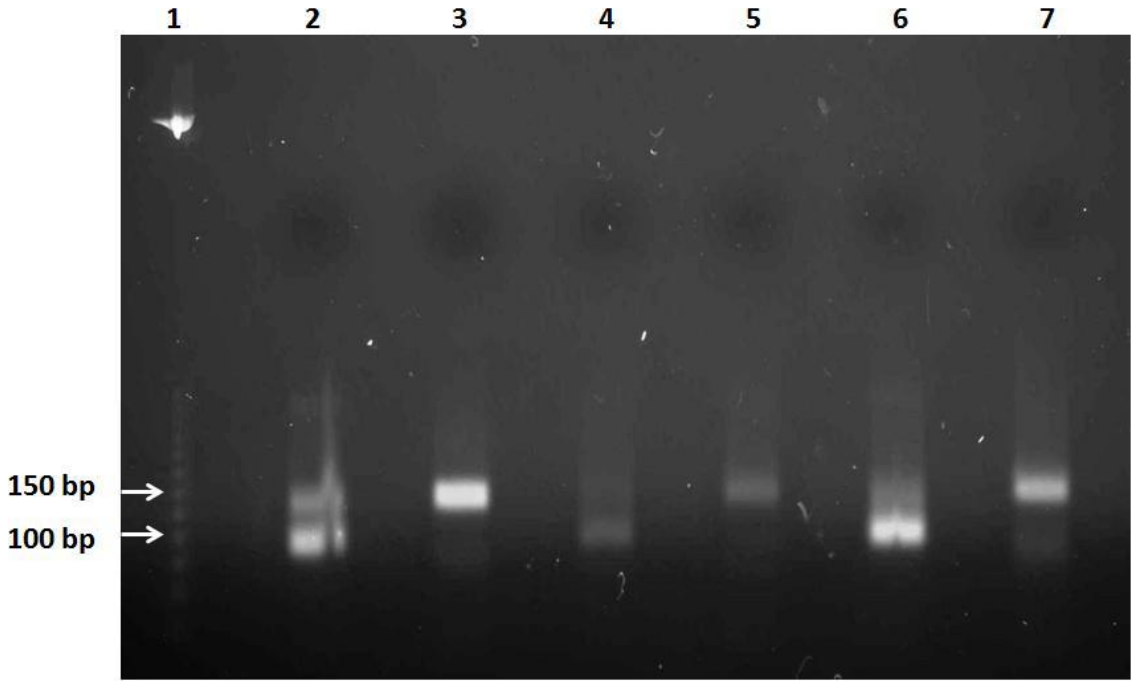

Figure 5: PCR amplification of the DpnII digest. 1) 25 bp DNA step ladder; 2) non-digested DNA P1 + P2 primers; 3) non-digested DNA P1 + P3 primers; 4) digested DNA heat-inactivated sample P1 + P2 primers; 5) digested DNA heat-inactivated sample P1 + P3 primers; 6) digested DNA precipitated sample P1 + P2 primers; 7) digested DNA precipitated sample P1 + P3 primers.

Figure 6 show that introduction of the previously described modifications improved PCR amplification. We were able to remove non-specific smears and additional bands representing undesirable PCR products that could be clearly seen in the previous agarose gels. Presence of the additional DNA bands in the digested samples with P1/P3 primers indicates that DpnII digest still didn't go to the completion, and thus after numerous PCR cycles, amplification of low amounts of the non-digested product is observed.

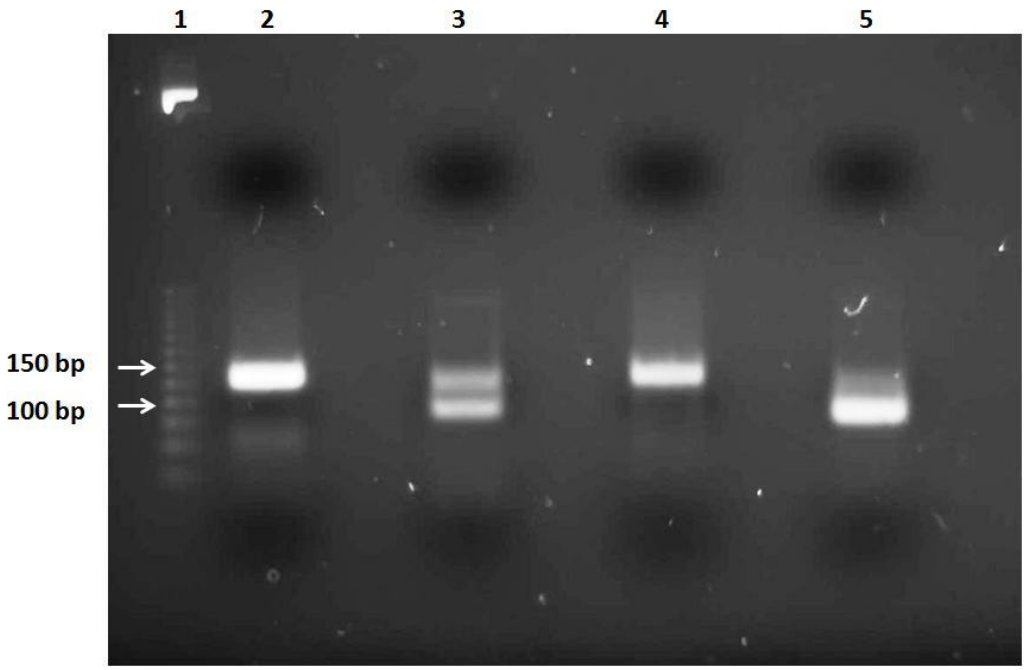

Figure 6: Modified PCR amplification of the DpnII digest. 1) 25 bp DNA step ladder; 2) non-digested DNA P1 + P3 primers; 3) non-digested DNA P1 + P2 primers; 4) digested DNA P1 + P3 primers; 5) digested DNA P1 + P2 primers.

In the previous experiment we concentrated our efforts on improving the PCR amplification, in the next step we worked on the enhancement of the DpnII digest to achieve better yields of digested DNA compared to the non-digested product. The reaction set up remained as before and digestion time was modified. Restriction digest was prolonged up to 16 h.

As it can be seen from **Figure 7** that we achieved better yields of the cut oligonucleotide, represented by bright DNA band of the proper molecular weight in the column #3. Since PCR amplification reached its maximum sensitivity, even a small copy of the non-digested product was amplified, which is represented by bands in the column #2. Non-specific bands, indicating presence of the additional PCR products are still present, which might be due to the non-specific binding of the selected primers that should be improved in the future experiments.

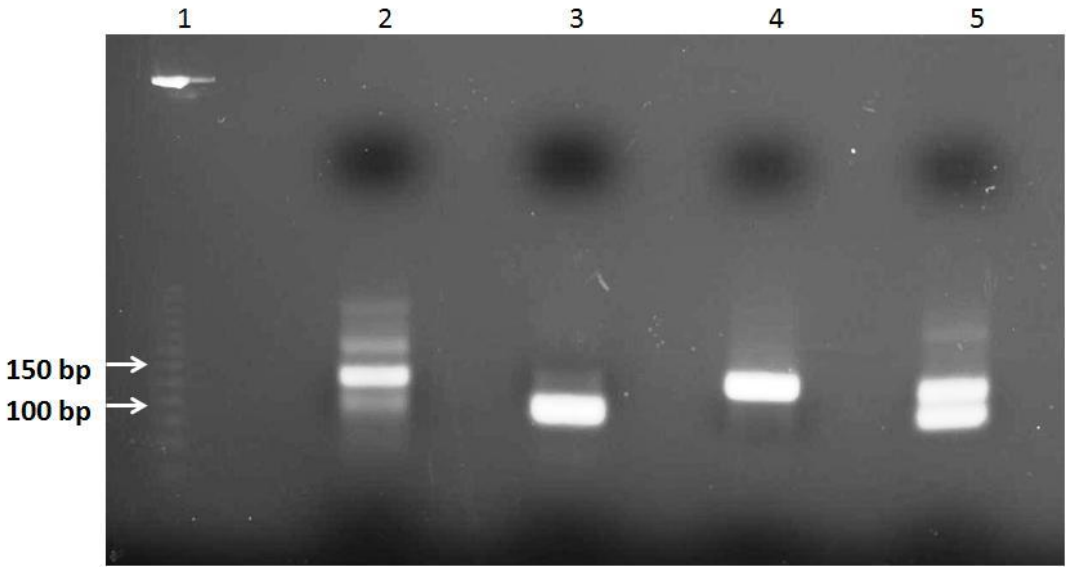

Figure 7: PCR amplification of the modified DpnII digest. 1) 25 bp DNA step ladder; 2) digested DNA P1 + P3 primers; 3) digested DNA P1 + P2 primers; 4) non-digested DNA P1 + P3 primers; 5) non-digested DNA P1 + P2 primers.

Based on these results we concluded that further improvements of this detection method would be time-consuming and potentially might not bring the desired out-come. For these reasons we decided to change PCR detection with visualization on agarose gels to quantitative real-time PCR analysis (qRT-PCR).

3.5 Quantitative real-time PCR analysis as a detection of the DpnII digest

After switching from regular PCR detection of the DpnII restriction digest to quantitative real-time PCR (qRT-PCR) several criteria had to be established. Among them – the quantity of the DNA for PCR amplification and the duration of the DpnII digest. Confirmation of the distinguishable difference of the cycle threshold (C_T) values between digested and non-digested DNA before performing hABH2 activity assay had to be determined. Cycle threshold – is a value, corresponding to the number of cycles at which the fluorescence signal from the PCR amplifications exceeds the selected for the experiment threshold.

Initial experiments were aimed at determining the proper amount of DNA to use to achieve good amplification range. qRT-PCR set-up and cycling conditions were as previously described.

Primers used for this qRT-PCR reaction were as following:

Forward primer (P1): 5' - TGTGCGTAAGGAAAAGTAAG – 3'

Reverse primer (P3): 5' – TCTTTCAGTCTCAAGACTCA – 3'

These primers were initially designed for the amplification of the non-digested copies of the oligonucleotide, but we realized that by adding those to the digested copies, qRT-PCR amplification should happen. Since digested product will have only one complementary primer C_T value for this sample will increase, because less quantity of the correct product will be formed and delay in the formation of the significant fluorescence signal will take place. Comparably, non-digested product will have two complementary primers leading to the exponential amplification of the DNA oligonucleotides that corresponds to low C_T value, since there is no delay in the detection of the fluorescence signal.

Based on the results represented in **Figure 8** we selected 1 pg of DNA input as a best example of C_T differences between the digested and non-digested DNA samples. These C_T values are detected in the middle of the 40 amplification cycles, which gives good scattering of the data.

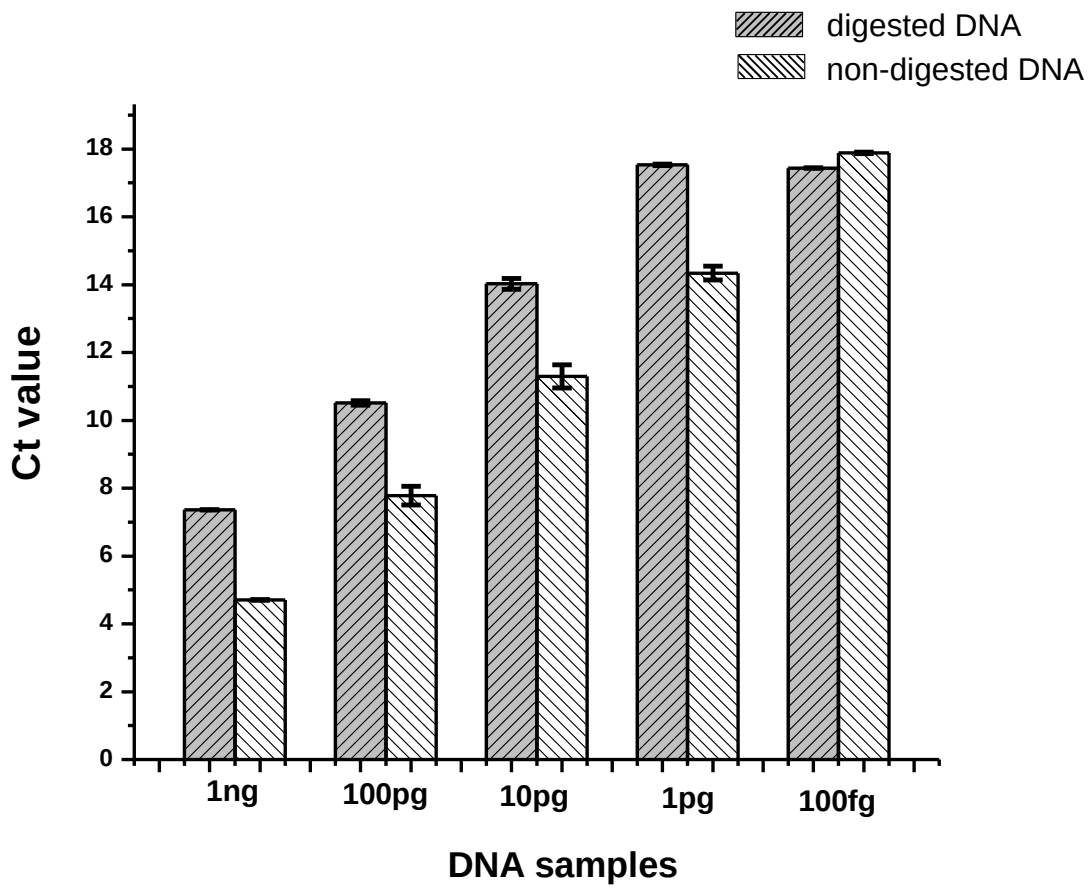

Figure 8: qRT-PCR amplification of the DpnII digest (DNA gradient).

After selection of the DNA input for qRT-PCR analysis we proceeded to the selection of the correct digestion time for DpnII reaction. Several short time periods and one long time period (16 h) were selected for this experiment. 16 h time point was selected based on the results from previous experiments. Digested DNA from all time points was compared to non-digested sample. qRT-PCR amplification set-up and cycling conditions were done as previously.

The biggest difference of the C_T values between digested and non-digested DNA was achieved for 16 h time point (**Figure 9**). These results match our previous data.

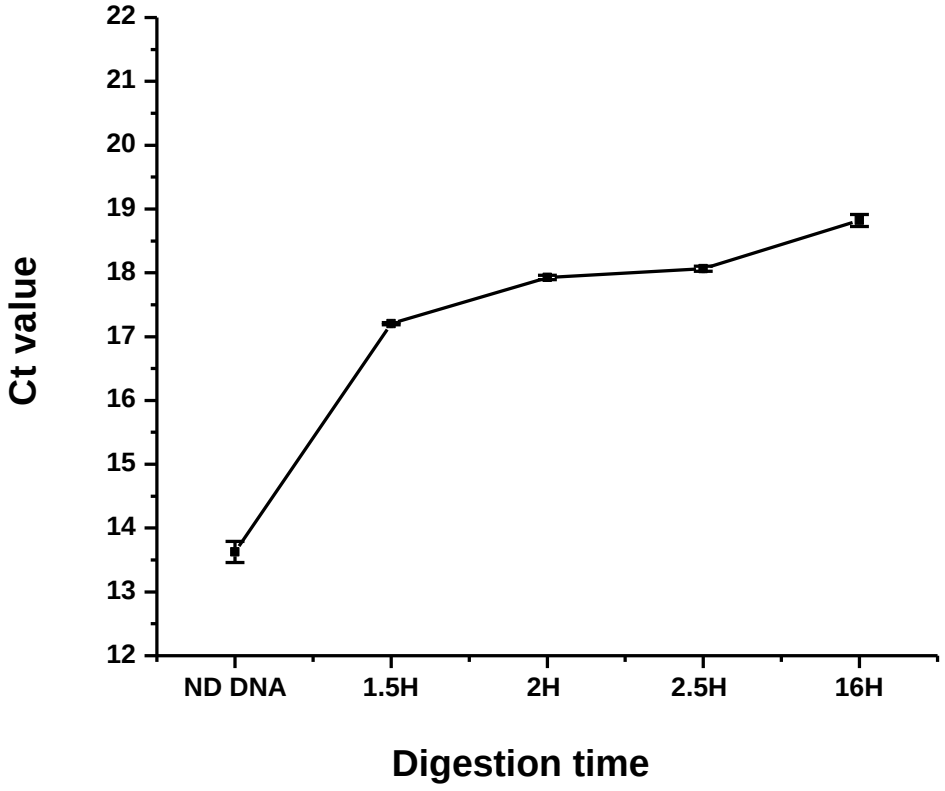

Figure 9: qRT-PCR amplification of the DpnII digest (Restriction digest time course).

After we determined the optimal amount of DNA for qRT-PCR amplification and exact DpnII digest conditions we proceeded with validation of the proposed detection method.

DpnII digest was set-up as previously with modified digestion time (16 h), all reagents were maintained the same. 1 pg of DNA was added to qRT-PCR reaction for amplification of the non-digested and DpnII digested DNA. Results are shown in **Figure 10**. We were able to achieve 4 cycles difference between two samples, which confirmed the applicability of this detection method for the measurement of the hABH2 activity.

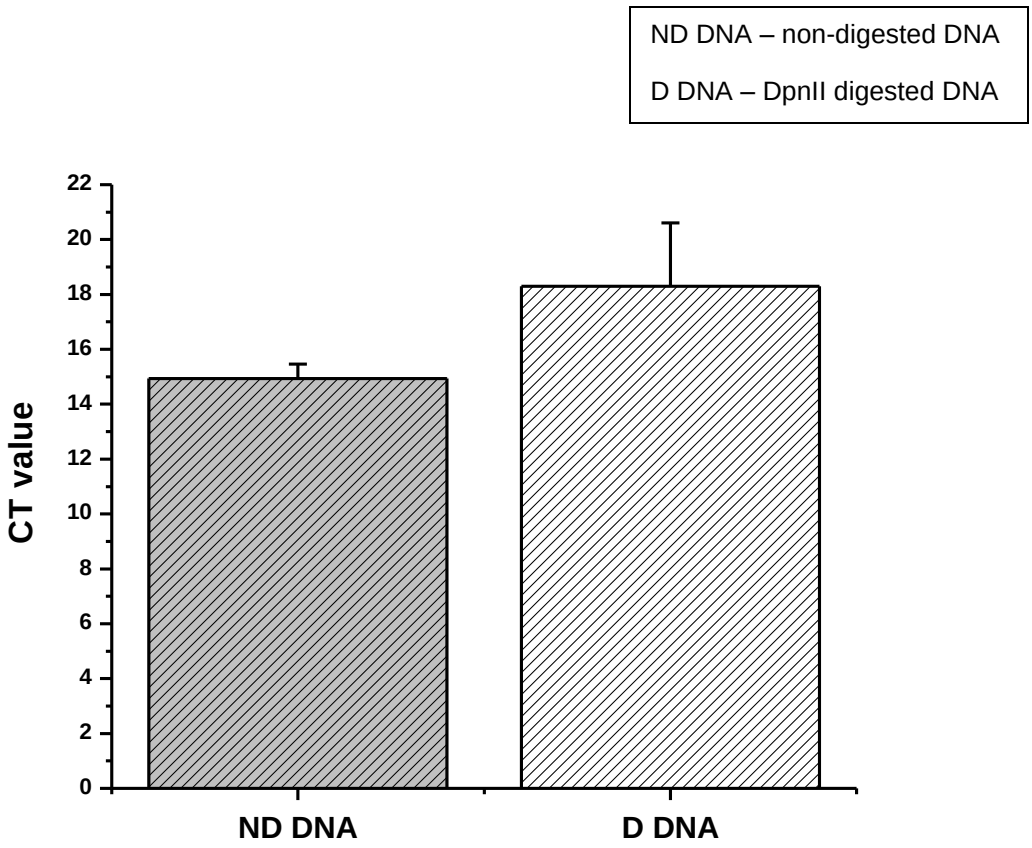

Figure 10: qRT-PCR amplification of the DpnII digest

3.6 qRT-PCR detection of the hABH2 activity

qRT-PCR detection of the DpnII digest on the specifically amplified region of the genomic DNA confirmed applicability of this method for future experiments on the hABH2 enzyme. Confirmation of the detection method made it possible to proceed with determination of the exact C_T values for regular DNA, methylated DNA and DNA after hABH2 assay. It was of great importance first to detect whether there are any differences in amplification between these three samples prior to the DpnII digest, since it potentially might eliminate non-necessary steps, which might bring fluctuations in the measurements. DNA samples that were used for this experiment were obtained in a different manner. Regular DNA was specifically amplified by means of the PCR analysis from the genomic sequence (exact sequence is shown below):

5’-TGTGCGTAAGGAAAAGTAAGGAAAACGATTCCTTCTAACAGAAATGTCCTGAGCA
ATCACCTATGAACTTGTTTCAAATGCAT**GATC**AAATGCAACCTCACAACCTTGGCTG
AGTCTTGAGACTGAAAGA-3’

Methylated DNA was purchased from GeneLink (Custom order) and had the same sequence as a regular DNA, with one exception. A cytosine in the DpnII recognition site (5’-GATC-3’) was replaced with a modified base – 3-methyl cytosine. The same methylated DNA was used for the hABH2 activity assay in a way as previously described. Since the major function of this enzyme is a removal of the methyl group from the 3rd position on cytosine, we expected that DNA after the hABH2 activity assay will have C_T values similar to the regular DNA, which is unmethylated. Also we expected to see higher C_T value for the methylated DNA since Taq DNA polymerase might have difficulties in the amplification of such oligonucleotide, due to the modification that prevents proper synthesis of the complementary strand. Regular DNA was expected to have lower C_T value, since it doesn’t have any obstacles for the amplification. qRT-PCR set-up was done as previously for DpnII digest, using 1 pg of DNA input and the same cycling conditions.

Figure 11 shows that our expectations were met and as it can be seen methylated DNA has the highest C_T value potentially due to the previously described difficulties in the amplification. Regular DNA has the lowest C_T value, which means there were no obstacles in the amplification of this oligonucleotide and DNA after hABH2 assay has the C_T value that is in between two previously mentioned samples. This indicates that hABH2 was able to remove the methyl group from the modified nucleobase on a portion of the oligonucleotides and it could be detected by our qRT-PCR method.

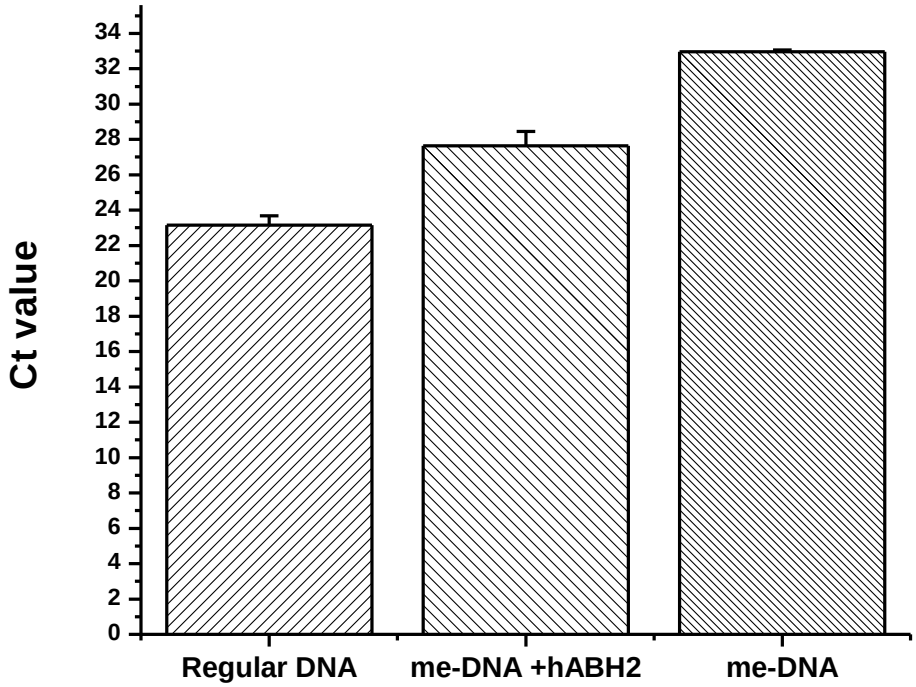

Figure 11: qRT-PCR amplification of the hABH2 assay – confirmation. Regular DNA – specifically amplified sequence of the genomic DNA; me-DNA+hABH2 – DNA after hABH2 assay; me-DNA – synthetically prepared DNA with one 3-me-dC incorporation.

Validation of our detection method linked to qRT-PCR analysis using regular DNA, methylated and DNA from hABH2 assay, showed that DpnII digest is not required and serves as an additional step that in the future can be avoided to make results more precise and consistent. As well, elimination of this step avoids additional external factors that might contribute to wrong or incomplete detection of the hABH2 activity.

Since the detection method was confirmed we proceeded to the next step – generation of the standard curve in order to determine the efficiency of the qRT-PCR reaction.

A standard curve was created with serially diluted DNA samples obtained from hABH2 assay as in the previous experiments. Samples were serially diluted by a factor of two starting at 0.25 ng and ending at 4 ng. This range was determined to be well within the detection level and

sensitivity of the qRT-PCR analysis. Average C_T values were plotted on a logarithmic scale against the log2 of the DNA concentration. Almost all amplifications demonstrated a linear relationship with DNA concentration. The resulting standard curve was used to calculate relative changes of the enzymatic activity in the control and samples treated with nitric oxide. Relative changes were converted to percentage of the displayed enzymatic activity in each experiment. Percentages were averaged, and SEM was calculated for each group. Data was presented as the mean of 5 SEM. The standard curve was:

$$y = 28.67819 + (-2.03912) * X \quad \text{(Adjusted } R^2\text{: 0.92243)} \quad \textbf{(Eq. 1)}$$

Efficiency of the oligonucleotide doubling with each cycle was:

$$E = (-1/\text{slope}) * 100\% \quad \textbf{(Eq. 2)}$$

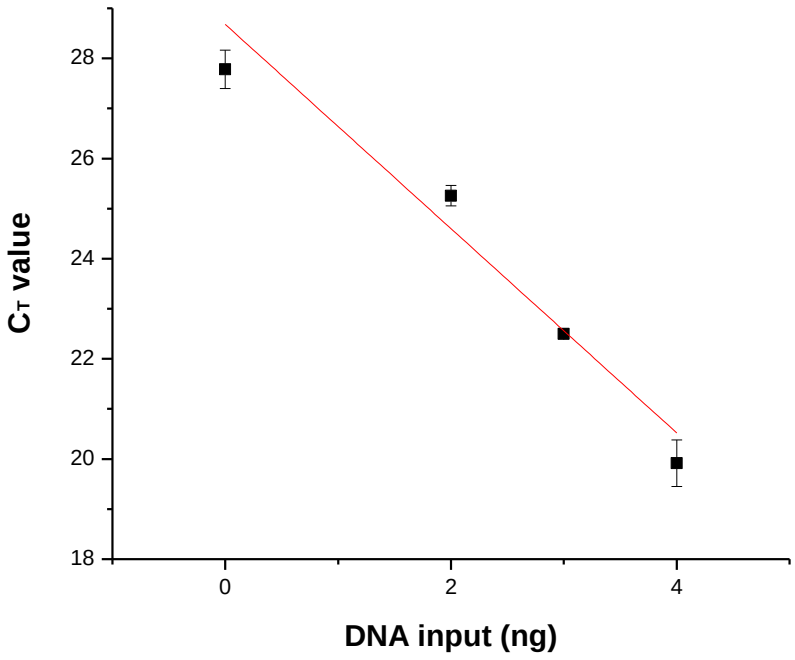

Figure 12: Standard curve representing efficiency of the qRT-PCR amplification of the DNA after hABH2 activity assay. Adjusted R^2 = 0.92243, intercept=28.67819 (SE=0.94969), slope= -2.03912 (SE= 0.33671).

In our case efficiency was 49 %. The resulting standard curve was used to calculate relative changes of the hABH2 activity in the controls and samples treated with nitric oxide according to the equation:

$$\text{Fold change} = 1.4^{-\Delta\Delta Ct} \quad (\textbf{Eq.3})$$

With the determined efficiency of the PCR reaction we proceeded to the development of the assay for the detection of the effects of nitric oxide on hABH2.

3.7 Detection of the nitric oxide effects on the hABH2 enzyme

Our initial steps confirmed that hABH2 activity assay linked to qRT-PCR analysis gives robust and reproducible results. The next goal was to apply this assay to detect direct inhibitory effects of nitric oxide on the enzyme. For this, experimental set-up of the hABH2 activity assay was followed. Nitric oxide treatments were done with 10 min pre-treatment with 100 µM spermine NONOate (Sper/NO). Sper/NO was added to the assay before the addition of DNA in order to prevent immediate demethylation of the DNA by hABH2. This enzyme is knows as an “ideal” enzyme, as it rapidly demethylates DNA. All co-factors and buffers were maintained at the required level. As a negative control we used a sample of methylated DNA, with all assay components, except for hABH2 enzyme.

After the assay time was over, the reaction was quenched as previously described and DNA from all three samples was subjected for qRT-PCR analysis, results of which are represented in **Figure 13**.

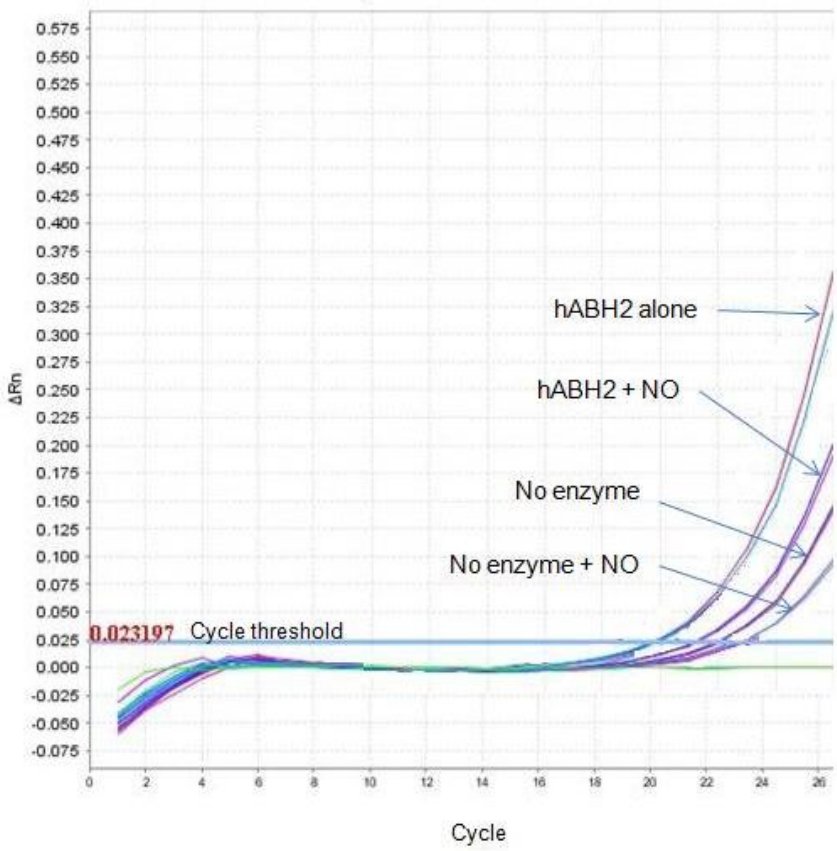

Figure 13: qRT-PCR amplification curves for hABH2 activity assay with controls. hABH2 – alone – DNA after hABH2 activity assay; hABH2+NO – DNA from hABH2 activity assay with 100 µM Sper/NO treatment; No enzyme – DNA from the control sample, which had all assay components except hABH2 enzyme; No enzyme + NO – DNA from the control sample, which had all assay components except hABH2 enzyme and 100 µM Sper/NO treatment.

Analysis of this data concluded that in the presence of NO· the product yield of demethylated DNA by hABH2 was 90% less than the amount in the absence of NO·. Values for the percentage change of the enzymatic activity of hABH2 alone and hABH2 + NO samples were normalized to the no enzyme sample (**Figure 14**). After performing unpaired *t* test statistical analysis the two-tailed P value was determined to be 0.0184. By conventional criteria, this difference is considered to be statistically significant. 95% confidence interval was used for this evaluation.

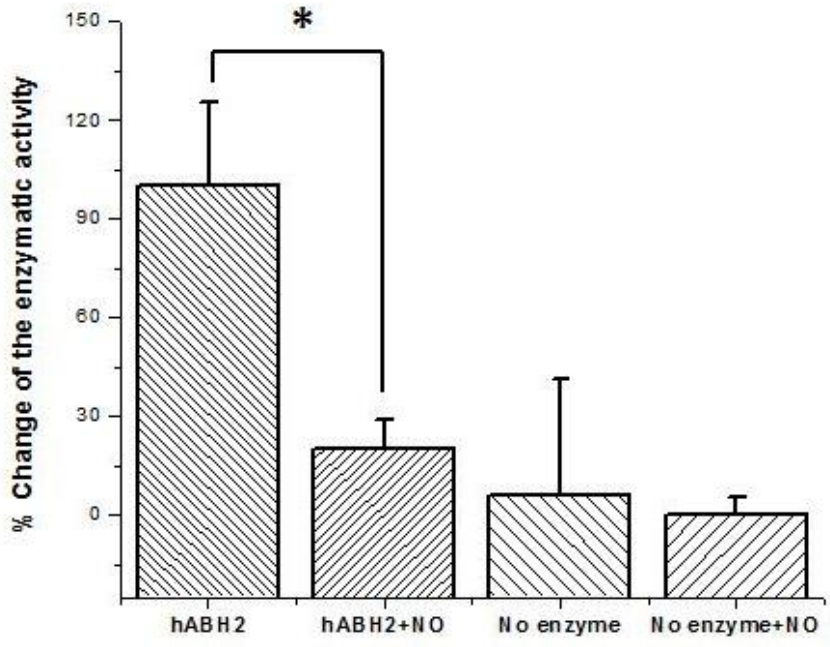

Figure 14: Effect of nitric oxide on hABH2 activity. hABH2 – value of the hABH2 activity from the non-treated sample; hABH2 + NO – value of the hABH2 activity after treatment with 100 µM Sper/NO; No enzyme – value for the negative control; No enzyme + NO – value for the negative control with 100 µM Sper/NO treatment. (*) – Difference in values for hABH2 activity and hABH2+NO activity are statistically significant.

4. DISCUSSION

This study was undertaken to gain insights into the molecular mechanisms of the interaction of nitric oxide with Fe(II)-dependent family of enzymes, particularly human AlkB homolog 2 (hABH2). Selection of hABH2 as a target for this research was based on the emerging interest to human homologs of *E.coli* AlkB enzyme (hABH group) as an adjuvant therapy for re-occurring or treatment-resistant neoplasias.

For a long time it was thought that nitric oxide's interaction with proteins was mainly limited to soluble guanylyl cyclase mechanism. Recently, our group showed that nitric oxide has a novel pathway for interactions with proteins – through chemical reactions with iron leading to the formation of dinitrosyl iron complexes (DNIC).

The hABH group of enzymes has an Fe(II) in the catalytical pocket for robust enzymatic activity. Thus we hypothesized, that nitric oxide could bind iron in the enzyme's active site by formation of dinitrosyl iron complexes, which would lead to the inhibition of hABH2 activity. We set out to test this hypothesis by detection and quantification of the hABH2 activity after nitric oxide treatment.

To-date the only method of detection for hABH2 activity is based on the use of radioactively labeled DNA. Major advantages of this method are: sensitivity and ability to produce robust and reproducible results. At the same time the amount of disadvantages prevails, such as: the need for specifically trained personnel, requirements for special safe handling and proper disposal of all materials used in the assay. Furthermore possibility of making this detection method automized is almost unrealistic, since it requires manual handling and therefore being used for low-throughput applications.

Keeping in mind all the drawbacks of radioactively labeled DNA detection method our first goal was to develop a novel methodology for hABH2 activity detection that will utilize advantages of the previously described method (sensitivity, ability to produce robust and

reproducible results) and at the same time will lack major disadvantages (special handling, safety issues, low-throughput application). As a result, the main objectives for the new methodology were: 1) reproducible results; 2) applicability for the future studies of the effects of nitric oxide; 3) sensitivity; 4) utilization of the techniques already developed in the lab.

We started the development of new methodology by preparing methylated DNA. Alkylating agent – methyl methanesulfonate (MMS) was used for this purpose. As has been previously shown (Wyatt and Pittman 2006), MMS can directly alkylate nucleobases positions which are determined by their nucleophilicity and by state of DNA itself, whether it is single-stranded or double-stranded molecule. We were interested in *N1*-adenine and *N3*-cytosine, since this are the locations acted upon by hABH2. *N*1-adenine and *N*3-cytosine are much more reactive as nucleophiles in the absence of hydrogen-bonding participation, that is, these two sites are much more susceptible to methylation in single stranded DNA (Wyatt and Pittman 2006) . We were unable to check the exact methylation status of the DNA after MMS treatment and did not know whether the desired positions on the nucleobases were methylated. Therefore we prepared two DNA set-ups for alkylation. The first set-up contained non-denatured DNA, which was in double-stranded state and second set-up had denatured DNA, which was in the single-stranded state. We then proceeded further with the detection part of the method, which involved agarose gel electrophoresis. After running the first few experiments it became obvious that this type of detection could not be used further since no difference in non-alkylated and alkylated samples was detected (Figure 1). Furthermore, the sample that we had the highest hopes for – denatured alkylated DNA didn't give any band, just a blurry trace, which made these results inconclusive. There are several possible explanations for such results (no re-annealing of the molecule after methylation, degradation of the DNA, *etc*). Although, we didn't confirm that the DNA molecule was actually methylated by methyl methanesulfonate we had enough theoretical background (Wyatt and Pittman 2006), to support this methodology. With this information we continued to use methyl methanesulfonate methylated DNA, but implemented a

different detection method, in hopes of achieving better differentiation between alkylated and non-alkylated samples.

Next approach at developing this assay was to use a fluorescence detection method. This technique is based on the generation of a fluorescence signal from the reaction of formaldehyde with the developing reagent provided in the activity detection kit. Formaldehyde is a sub-product of hABH2 demethylation reaction. Initially the results that we were receiving looked very promising (Figure 2). Notable difference could be seen between non-denatured alkylated DNA after hABH2 assay and denatured alkylated DNA after hABH2 assay. Particularly interesting were the results from denatured samples after hABH2 assay – higher amount of fluorescence signal was detected. This initially looked like confirmation of our ideas about higher nucleophilic potential of the denatured DNA for the alkylation on the adenines and cytosines. After few more experiments were done striking trends in the results could be seen. Unfortunately, the untreated sample (unmethylated) was giving the highest fluorescence signal, comparably to others (Figure 3). Since we were unable to reduce this background signal we had to terminate future use of this detection method for our experiments.

Since the previous methods couldn't confirm the level of DNA methylation, or the exact positions that were methylated we decided to further change the detection method and switch to a restriction enzyme digest approach.

DpnII is a methylation sensitive restriction enzyme that recognizes sequence 5'-GATC-3' in the oligonucleotides. This restriction enzyme is inhibited if either adenine or cytosine is methylated in the recognition sequence. After specific amplification by means of PCR analysis, oligonucleotides containing the recognition sequence were obtained from the genomic DNA, previously extracted from cancer cells. The restriction digest was run as previously described followed by PCR analysis with specially designed primers. All together we used three primers. Primer P1 started amplification of the 5' end of the non-digested and digested oligonucleotide, since they are identical. Primer P2 amplified 3' end of the digested oligonucleotide and Primer

P3 amplified 3' end of the non-digested oligonucleotide. At the initial experiments we used to add all three primers into one reaction vial for digested and non-digested samples, but afterwards we realized that such set-up gave un-characterized smears on the agarose gel that prevented proper evaluation of the results.

In the next step, we divided primers P1 + P2 and P1 + P3 into two different reaction vials. We expected that results would be as following: digested oligonucleotide would be represented by a band corresponding to the PCR product amplified by P1 + P2 primers and no band would be detected for the PCR product amplified by P1 + P3 primers or at least a notable difference in terms of intensity of the bands would be present. Presence of the band, corresponding to the PCR product amplified by P1 + P3 primers on the digested oligonucleotide would mean that restriction digest didn't go to the completion and even a low copy of the non-digested oligonucleotide was amplified. For the non-digested oligonucleotide we expected to see two intensive bands since both places for primers annealing are still present on the DNA.

First experiments using such set-up provided us with promising data, even though two bands were still present for the digested oligonucleotide (Figure 5). We were able to see a difference between them in terms of bands intensity. As well, the digested samples were quite different from the non-digested ones. After several cycles of optimization of the experimental conditions, we were able to improve the resolution quality of the agarose gel representation and increase the difference in band intensity between digested and non-digested samples (Figure 7). Unfortunately we were un-able to improve the technique further and eliminate the band with P1 + P3 primers for the digested oligonucleotide. As these results, were still unsatisfactory, we decided to switch to a different experimental set-up using quantitative real-time PCR analysis (qRT-PCR) as a detection tool.

Set-up for qRT-PCR was done as previously described. Selection of primers for qRT-PCR analysis was done differently than for regular PCR analysis. For the amplification we used only primers P1 and P3. Our major goal for using qRT-PCR as a detection tool was to measure

amplification differences between DpnII digested and non-digested DNA. Polymerase chain reaction is an exponential amplification of the DNA input, when all components are provided in the correct quantity and concentration. As it was previously described, primers P1 and P3 were designed for the non-digested DNA oligonucleotide. By using them for the digested samples, we would observe complementarity only for primer P1, and not for P3. Hence we expected that observed amplification for the digested oligonucleotide would be somewhere in the range between linear to strongly impaired exponential amplification, which can be well characterized by the C_T value. With the optimization experiments, we were able to determine the correct quantities of the DNA for the qRT-PCR set-up and the best digestion time for the DpnII reaction (Figure 8-9). These results led us to confirm that DpnII digest linked to qRT-PCR analysis could be used as a detection tool for the measurement of the hABH2 activity. Therefore, this method could be used for the future experiments to determine effects of nitric oxide on hABH2.

After assay optimization we moved on to trying to determine the effect of nitric oxide on hABH2 activity. For this we purchased synthetically generated DNA oligonucleotide that had a single modified insertion (3-methyl cytosine) in the 5'-GATC-3' restriction sequence. With this modification we were able to detect activity of the hABH2 by means of DpnII restriction digest since it is located in the recognition sequence for this enzyme. As a detection method we continued using qRT-PCR technique.

Before starting with DpnII digest we decided to verify whether methylated DNA itself would have a different trend in amplification compared to a non-methylated and DNA after hABH2 activity assay. We were able to see 4-5 cycles of amplification difference between these three samples, since DNA polymerase cannot easily replicate methylated DNA. This led to the elimination of the DpnII digestion step as an un-necessary one (Figure 11). Such improvements made our method more precise, since removal of this additional step eliminated reasons for the additional mistakes within the process. It also removed potential side effects from the restriction digest itself, which might alter detection of the amplification signal. After generation of the

standard curve we concluded that efficiency of our qRT-PCR reaction is 49%. In general, such efficiency is low and potentially doesn't represent the amplification power of our reaction to the full extend. We moved on to measuring the effects of nitric oxide on hABH2. To measure effects of this free radical on the hABH2 we set up the hABH2 activity assay, which included all the required components (ascorbate, α-ketoglutarate, $FeSO_4$, $MgCl_2$ and Tris/HCl). Nitric oxide treatments were done in the form of 10 min pre-treatment with 100 μM spermine NONOate – Sper/NO, which was added to the assay before DNA addition in order to prevent direct function of the hABH2 enzyme. All co-factors and buffers were maintained on the required level to insure that inhibition of hABH2 is due to the nitric oxide effects and not because of lack of necessary cofactors or substrates. As a negative control we used a sample of methylated DNA containing all necessary components of the assay, except for hABH2 enzyme.

Immediately after enzymatic reaction was over it was quenched and the DNA was prepared for qRT-PCR analysis. The DNA and primers concentrations were calculated based on the results from the optimization experiments. The data received from multiple experiments strongly suggest that in the presence of NO· the product yield of demethylated DNA by hABH2 was 90% less than the amount in the absence of NO· (Figure 12). Such results support our initial hypothesis. The next step in this project would be to confirm that nitric oxide inhibits hABH2 through our proposed mechanism - binding iron at the catalytical site. So far, the initial electro paramagnetic resonance (EPR) experiments that were conducted to support this hypothesis indicate that this mechanism may be responsible for the inhibitory effects of NO· on the hABH2 activity.

5. CONCLUSIONS AND FUTURE DIRECTIONS

In the present work, we developed a novel method to measure hABH2 demethylation activity using quantitative real-time PCR. We demonstrated that in the presence of NO· the product yield of demethylated DNA by hABH2 was 90% less than the amount in the absence of NO·.

In order to establish an accurate detection technique, several methods were attempted: agarose gel electrophoresis, fluorimetirc assay, DpnII restriction digest linked with regular PCR and finally quantitative real-time PCR analysis linked with hABH2 activity assay. The latter detection method was developed specifically for this project and hence was the selected method for this research. The unique and characteristic feature of the current method lies in the ability to take advantage of the previously known detection methods, in terms of sensitivity and reproducibility of the results while avoiding major drawbacks of radioactive assay that includes radioactive contamination, specially trained personal, etc.

Previously it was shown that nitric oxide even at low concentrations is able to effectively bind iron, like from the cellular chelatable iron pool. This project expanded our understanding on the ability of nitric oxide to bind iron found in the catalytical pockets of non-heme proteins. Such observations will open new venues of research and steer further scientific studies toward investigating the different effects of nitric oxide on Fe(II) dependent enzymes which possess diverse biological functions.

Future directions for the current project will be focused on determining the actual mechanism of inhibition exerted by nitric oxide on hABH2 functional activity. One of the possible scenarios for the observed results is the formation of paramagnetic nitrosyliron species. This outcome is based on previously reported observation of the formation of dinitrosyl-iron complexes by Dr. Thomas group. To validate proposed hypothesis *in vitro* experiments with

recombinant hABH2 and nitric oxide will be performed with the help of EPR spectroscopy. So far, preliminary results are providing a promising starting point for further investigations to validate the current hypothesis. As part of our future plan, we will initiate ligand based and structure based drug design efforts to discover potential compounds that can harness this new mechanism of inhibition by nitric oxide using the newly developed assay described herein.

CITED LITERATURE

Aas, P. A., M. Otterlei, et al. (2003). "Human and bacterial oxidative demethylases repair alkylation damage in both RNA and DNA." Nature **421**(6925): 859-863.

Aravind, L. and E. V. Koonin (2001). "The DNA-repair protein AlkB, EGL-9, and leprecan define new families of 2-oxoglutarate- and iron-dependent dioxygenases." Genome Biol **2**(3): RESEARCH0007.

Barlow, D. P. (2011). "Genomic imprinting: a mammalian epigenetic discovery model." Annu Rev Genet **45**: 379-403.

Barreto, G., A. Schafer, et al. (2007). "Gadd45a promotes epigenetic gene activation by repair-mediated DNA demethylation." Nature **445**(7128): 671-675.

Bignami, M., M. O'Driscoll, et al. (2000). "Unmasking a killer: DNA O(6)-methylguanine and the cytotoxicity of methylating agents." Mutat Res **462**(2-3): 71-82.

Boiteux, S. and J. Laval (1982). "Mutagenesis by alkylating agents: coding properties for DNA polymerase of poly (dC) template containing 3-methylcytosine." Biochimie **64**(8-9): 637-641.

Brockdorff, N. (2011). "Chromosome silencing mechanisms in X-chromosome inactivation: unknown unknowns." Development **138**(23): 5057-5065.

Chen, B., H. Liu, et al. (2010). "Mechanistic insight into the recognition of single-stranded and double-stranded DNA substrates by ABH2 and ABH3." Mol Biosyst **6**(11): 2143-2149.

Dodson, M. L., M. L. Michaels, et al. (1994). "Unified catalytic mechanism for DNA glycosylases." J Biol Chem **269**(52): 32709-32712.

Duncan, T., S. C. Trewick, et al. (2002). "Reversal of DNA alkylation damage by two human dioxygenases." Proc Natl Acad Sci U S A **99**(26): 16660-16665.

Falnes, P. O., M. Bjoras, et al. (2004). "Substrate specificities of bacterial and human AlkB proteins." Nucleic Acids Res **32**(11): 3456-3461.

Flores-Santana, W., C. Switzer, et al. (2009). "Comparing the chemical biology of NO and HNO." Arch Pharm Res **32**(8): 1139-1153.

Gehring, M., W. Reik, et al. (2009). "DNA demethylation by DNA repair." Trends Genet **25**(2): 82-90.

Hickok, J. R., S. Sahni, et al. (2011). "Dinitrosyliron complexes are the most abundant nitric oxide-derived cellular adduct: biological parameters of assembly and disappearance." Free Radic Biol Med **51**(8): 1558-1566.

Hickok, J. R. and D. D. Thomas (2010). "Nitric oxide and cancer therapy: the emperor has NO clothes." Curr Pharm Des **16**(4): 381-391.

Huang, J. C., D. S. Hsu, et al. (1994). "Substrate spectrum of human excinuclease: repair of abasic sites, methylated bases, mismatches, and bulky adducts." Proc Natl Acad Sci U S A **91**(25): 12213-12217.

Huang, J. C. and A. Sancar (1994). "Determination of minimum substrate size for human excinuclease." J Biol Chem **269**(29): 19034-19040.

Ignarro, L. J. (1996). "Physiology and pathophysiology of nitric oxide." Kidney Int Suppl **55**: S2-5.

Kim, J. K., M. Samaranayake, et al. (2009). "Epigenetic mechanisms in mammals." Cell Mol Life Sci **66**(4): 596-612.

Kurowski, M. A., A. S. Bhagwat, et al. (2003). "Phylogenomic identification of five new human homologs of the DNA repair enzyme AlkB." BMC Genomics **4**(1): 48.

Larson, K., J. Sahm, et al. (1985). "Methylation-induced blocks to in vitro DNA replication." Mutat Res **150**(1-2): 77-84.

Law, J. A. and S. E. Jacobsen (2010). "Establishing, maintaining and modifying DNA methylation patterns in plants and animals." Nat Rev Genet **11**(3): 204-220.

Mishina, Y. and C. He (2006). "Oxidative dealkylation DNA repair mediated by the mononuclear non-heme iron AlkB proteins." J Inorg Biochem **100**(4): 670-678.

Monk, M., M. Boubelik, et al. (1987). "Temporal and regional changes in DNA methylation in the embryonic, extraembryonic and germ cell lineages during mouse embryo development." Development **99**(3): 371-382.

Morey, C. and P. Avner (2011). "The demoiselle of X-inactivation: 50 years old and as trendy and mesmerising as ever." PLoS Genet **7**(7): e1002212.

Muller, T. A., K. Meek, et al. (2010). "Human AlkB homologue 1 (ABH1) exhibits DNA lyase activity at abasic sites." DNA Repair (Amst) **9**(1): 58-65.

Ringvoll, J., M. N. Moen, et al. (2008). "AlkB homologue 2-mediated repair of ethenoadenine lesions in mammalian DNA." Cancer Res **68**(11): 4142-4149.

Sancar, A. (1995). "DNA repair in humans." Annu Rev Genet **29**: 69-105.

Sedgwick, B. (2004). "Repairing DNA-methylation damage." Nat Rev Mol Cell Biol **5**(2): 148-157.

Smiley, J. A., M. Kundracik, et al. (2005). "Genes of the thymidine salvage pathway: thymine-7-hydroxylase from a Rhodotorula glutinis cDNA library and iso-orotate decarboxylase from Neurospora crassa." Biochim Biophys Acta **1723**(1-3): 256-264.

Suzuki, M. M. and A. Bird (2008). "DNA methylation landscapes: provocative insights from epigenomics." Nat Rev Genet **9**(6): 465-476.

Thomas, D. D., L. A. Ridnour, et al. (2006). "Superoxide fluxes limit nitric oxide-induced signaling." J Biol Chem **281**(36): 25984-25993.

Thomas, D. D., L. A. Ridnour, et al. (2008). "The chemical biology of nitric oxide: implications in cellular signaling." Free Radic Biol Med **45**(1): 18-31.

Toledo, J. C., Jr., C. A. Bosworth, et al. (2008). "Nitric oxide-induced conversion of cellular chelatable iron into macromolecule-bound paramagnetic dinitrosyliron complexes." J Biol Chem **283**(43): 28926-28933.

Wink, D. A. and J. B. Mitchell (1998). "Chemical biology of nitric oxide: Insights into regulatory, cytotoxic, and cytoprotective mechanisms of nitric oxide." Free Radic Biol Med **25**(4-5): 434-456.

Wu, S. C. and Y. Zhang (2010). "Active DNA demethylation: many roads lead to Rome." Nat Rev Mol Cell Biol **11**(9): 607-620.

Wyatt, M. D. and D. L. Pittman (2006). "Methylating agents and DNA repair responses: Methylated bases and sources of strand breaks." Chem Res Toxicol **19**(12): 1580-1594.

VITA

NAME: Yuliya Mikhed

EDUCATION: BSc., Pharmacy, National University "Lvivska Politechnika", Lviv, Ukraine, 2008

MSc., Medicinal chemistry, University of Illinois at Chicago, Chicago, IL, 2012

MEMBERSHIP: Society of the Free Radical Biology and Medicine (SFRBM)

American Association of Pharmaceutical Students (AAPS)

ABSTRACTS: **Y.Mikhed**, J.R. Hickok, D.D. Thomas. Oxygen regulates nitric oxide mediated signaling by determining the rate of synthesis and metabolism of nitric oxide. (Poster). The 18th National meeting of the Society of Free Radical Biology and Medicine, Atlanta, GA, 2011.

PUBLICATIONS: J.R. Hickok, S. Sahni, **Y. Mikhed**, M.G. Bonini, D.D. Thomas. Nitric oxide suppresses tumor cell migration through N-Myc downstream-regulated gene-1 (NDRG1) expression: role of chelatable iron. J Biol Chem. 2011 Dec 2;286(48):41413-24

AWARDS: B.Sc. with honors, Ukraine, 2008

J. William Fulbright Foreign Scholarship award, Ukraine, 2009

Graduate Student Council Travel Award, Chicago, IL, 2011

UIC Young Presenter Award, Chicago, IL, 2012